Supplementary information

Discovery of a novel class of dual GPBAR1 Agonists-RORγt inverse agonists for the treatment of IL-17 mediated disorders

Bianca Fiorillo,[1, ‡] Rosalinda Roselli,[1, ‡] Claudia Finamore,[1, ‡] Michele Biagioli,[2,*] Cristina di Giorgio,[2] Martina Bordoni,[3] Paolo Conflitti,[4] Silvia Marchianò,[2] Rachele Bellini,[2] Pasquale Rapacciuolo,[1] Chiara Cassiano,[1] Vittorio Limongelli,[1,4] Valentina Sepe,[1,*] Bruno Catalanotti,[1] Stefano Fiorucci,[2] and Angela Zampella[1]

[1] Department of Pharmacy, University of Naples "Federico II", Via D. Montesano, 49, I-80131 Naples, Italy

[2] Department of Medicine and Surgery, University of Perugia, Piazza L. Severi 1-06132 Perugia, Italy

[3]Precision BioTherapeutics, SrL, Perugia, Italy

[4] Università della Svizzera italiana (USI), Faculty of Biomedical Sciences, Euler Institute, via G. Buffi 13, CH-6900 Lugano, Switzerland

Table of contents

Table S1. Efficacy on FXR -LXRα/β

	FXR [a]	FXR [b]	LXRα [c]	LXRβ [c]
Compound **3**	21.0 ± 0.3	14.5 ± 2.2	10.6 ± 1.5	11.8 ± 1.6
Compound **7**	31.6 ± 7.8	14.7 ± 2.0	14.6 ± 0.8	13.9 ± 0.6

[a]Efficacy (Eff. %) is the efficacy of the compound (10 μM) relative to **CDCA** (10 μM) as 100. [b]Efficacy (Eff. %) is the efficacy of the compound (10 μM) relative to **CDCA** (10 μM) as 100, calculated in Alphascreen-based cofactor recruitment assay. [c]Efficacy (Eff. %) is the efficacy of the compound (10 μM) relative to **GW3965** (10 μM) as 100.

Docking calculation.

The best binding poses of **3** and **7** to RORγ were similar with respect to the co-crystallized ligands.[1,2] The tetracyclic core of **3** was placed in the amphipathic pocket between helices (H) H4 and H5, where it was further stabilized by a set of hydrophobic interactions with the side chains of Leu287, Val361, Val376, and Phe378 (Figure S1, panel A). The hydroxy group at C-3 made a H-bond with Gln286 on H1, whereas the flexible chain at C-17 bent slightly to better adapt to the pocket formed by H4, H8, H11, and H12. The methylene portion on the side chain at C-17 made hydrophobic interactions with Phe388, Ile397, and Ile400, while the ethereal oxygen at C-24 H-bonded Cys320. The aromatic ring protruded towards H11, in the amphipathic pocket formed by H4, H8, H11, and H12, establishing hydrophobic interactions with Leu324 and Leu391 and a T-shaped π interaction with Trp317 (Figure S1, panel A). Finally, the *para*-carboxylic group took contact with His479. Compound **7** showed the same pattern of interactions as **3** (Figure S1). However, the *meta*-hydroxymethylene group made additional H-bonds with the backbone of Trp317 and with the side chain of Tyr502 (Figure S1, panel B).

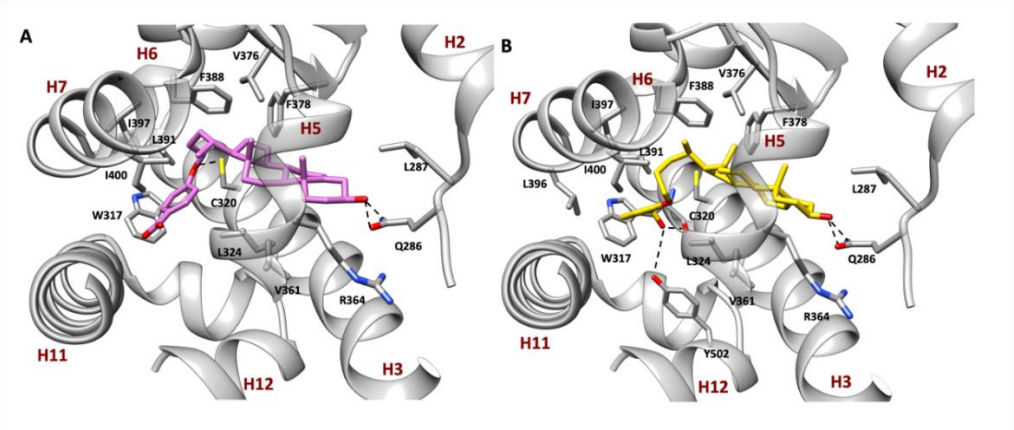

Figure S1. Docking poses of (A) **3** and (B) **7** against RORγ. Ligands are represented as *pink* and *gold* sticks, respectively, whereas the interacting residues of the receptor are shown in *gray* and labelled. Oxygen atoms are depicted in *red* and nitrogens in *blue*. The receptor is represented as ribbons with its helices (H) labelled. Hydrogens are omitted for the sake of clarity and H-bonds are displayed as dashed black lines.

It is noteworthy that docking calculations on the corresponding derivatives **15** and **16**, bearing the *cis* A/B junction (bile acid-like), showed a different binding mode. The non-planar structure, located in the same pocket, determined a rotation of the steroid nucleus leading to the weakening of the hydrophobic interaction, but also inducing a different orientation of the side chain at C-17. In this way, the aromatic ring is placed in a very limited region, close to Trp317 and Tyr502, where only the small linear nitrile function of compound **17** can fit. Moreover, with respect to compounds belonging to the first subset, the α-configuration of the hydroxyl group at C-3 led to the loss of the H-bond with Gln286, as also showed by the lower Glide score (Figure S2). This finding is in full agreement with the low efficacy of RORγ inverse agonists demonstrated by compounds **15** and **16**.

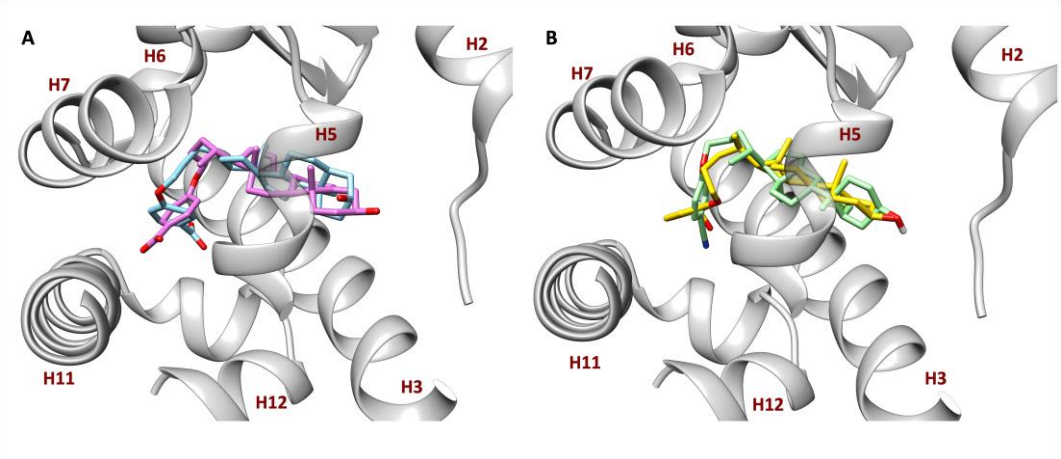

Figure S2. Superimposed binding mode of (A) **3** (in *pink*) and **16** (in *light blue*) and (B) **7** (in *yellow*) and **19** (in *light green*) against RORγ. Oxygen atoms are depicted in *red* and nitrogens in *blue*. The receptor is represented as ribbons with its helices (H) labelled. Hydrogens are omitted for the sake of clarity.

Docking calculations showed that **3** and **7** binding modes to GPBAR1 (Figure S3) were similar to other, recently discovered bile acids endowed with agonistic activity.[3–5] Compound **3** steroidal scaffold was placed in the amphipathic pocket between transmembrane helices (TM) 3, 5, and 6, formed by Tyr89, Asn93, Phe96, Phe138, Leu162, Glu169, Trp237, and Tyr240, where it made hydrophobic interactions with Phe96, Phe138, and Leu162. Moreover, the hydroxyl group at C-3 made a H-bond with the backbone of Glu169, which is known to be involved in the binding of agonists and receptor activation.[4,6] The flexible side chain at C-17 extended towards TM1 and TM2,

determining hydrophobic interactions between the methylene linker, Leu71 and Leu266. The aromatic portion at C-24, pointing to TM1, took contacts with Ser21 and Ser270. Finally, the carboxyl group H-bonded Trp75 (Figure S3, panel A). Also docking calculations performed in GPBAR1 showed that the binding mode of compound **7** was similar to **3** with the difference in the hydroxyl terminal group, which made a H-bond with the backbone of Leu68 (Figure S3, panel B). Moreover, the steroidal scaffold made hydrophobic contacts also with Leu97, while the aromatic group with Leu71 and Leu74.

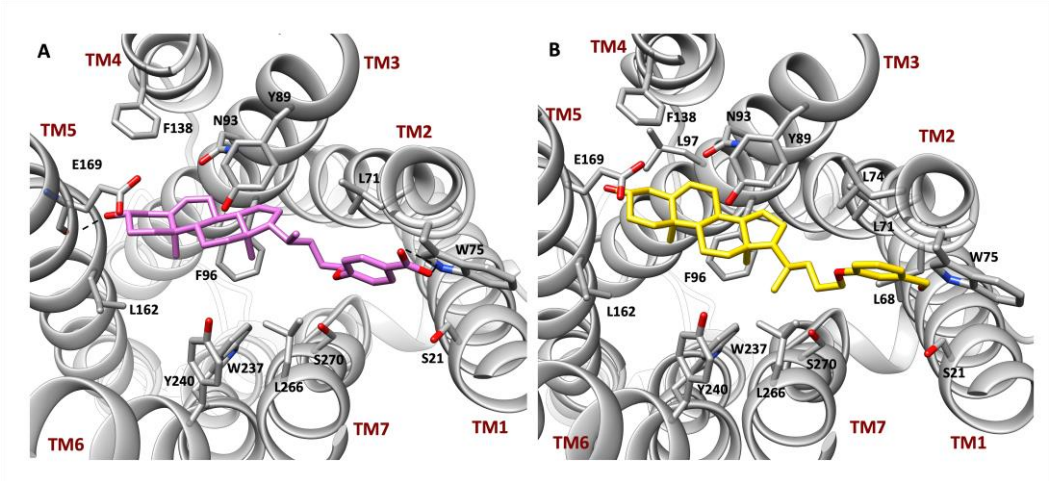

Figure S3. Binding mode of (A) **3** and (B) **7** in GPBAR1. Ligands are represented as *pink* and *gold* sticks, respectively, whereas the interacting residues of the receptor are shown in *grey* and labelled. Oxygen atoms are depicted in *red* and nitrogens in *blue*. The receptor is represented as ribbons with its transmembrane helices (TM) labelled. Hydrogens are omitted for the sake of clarity and H-bonds are displayed as dashed lines.

The result of 500 ns of MDs of the co-crystallized agonist ligand - 22R-hydroxycholesterol - in the active form of RORγ (PDB ID 3l0j)[1] showed a stable binding mode, maintained over all the simulation time (RMSD = 0.22 Å and 0.12 Å, calculated on ligand's heavy atoms and on the protein backbone, respectively) (Figure S4). Additionally, considering that compounds **3** and **7** interacted with the key residues' pathway involved in the mechanism of activation/deactivation of the receptor, destroying the H-bond network between His479 and Tyr502 on H11 and H12, respectively, and stabilizing the open and inactive form of H12, here the co-crystallized agonist ligand - 22R-hydroxycholesterol – stabilized H12 in the closed and active conformation, preserving the H-bond between His479 and Tyr502 (Figure S5).

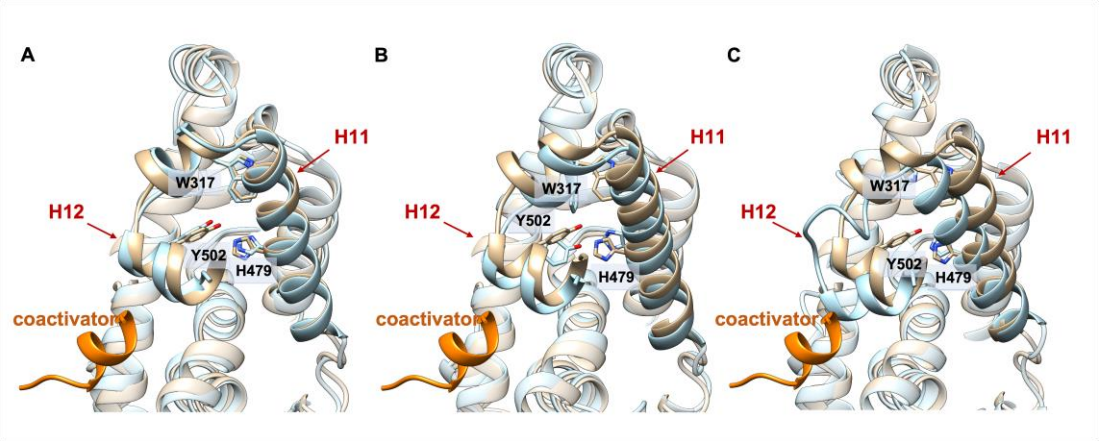

Figure S4. Superimposition of the X-ray structure of RORγ (PDB ID 3l0j)[1] (in *tan* cartoon) and the MDs last frame of A) the co-crystallized agonist ligand 22(R)-Hydroxycholesterol, B) compound **3** and C) compound **7** in complex with RORγ (in *cyan* cartoon). The coactivator is represented in orange cartoon. Key residues are represented in sticks and labelled.

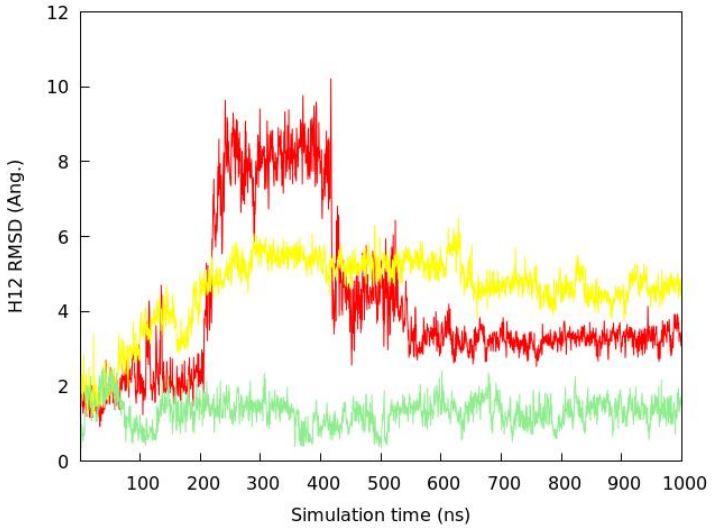

Figure S5. Plots of average RMSD calculated on the H12 residues backbone (Pro500-Ser507) of RORγ in complex with compounds **3** (in red), **7** (in *yellow*) and the co-crystallized agonist ligand 22(R)-Hydroxycholesterol (in *light green*).

Experimental Section

Chemistry. High-resolution electrospray ionization mass spectrometry (ESI-MS) spectra were performed with an LTQ-XL equipped with an Ultimate 3000 HPLC system (Thermo Fisher Scientific) mass spectrometer. NMR spectra were obtained on a Bruker 400 spectrometer (^{1}H at 400, ^{13}C at 100 MHz), recorded in $CDCl_3$ (δ_H = 7.26 and δ_C = 77.0 ppm) and CD_3OD (δ_H = 3.30 and δ_C = 49.0 ppm). Detected signals were in accordance with the proposed structures. Coupling constants (J values) are given in hertz (Hz), and chemical shifts (δ) are reported in ppm and referred to CHD_2OD and $CHCl_3$ as internal standards. Spin multiplicities are given as s (singlet), br s (broad singlet), d (doublet), t (triplet), or m (multiplet).

HPLC was performed with a Waters model 510 pump equipped with Waters Rheodine injector and a differential refractometer, model 401. Reaction progress was monitored via thin-layer chromatography (TLC) on Alugram silica gel G/UV254 plates. Silica gel MN Kieselgel 60 (70–230 mesh) from Macherey-Nagel Company was used for column chromatography. All chemicals were obtained from Zentek, Inc.

Silica gel (200–400 mesh) from Macherey-Nagel Company was used for flash chromatography. All chemicals were obtained from Sigma-Aldrich, Inc. Solvents and reagents were used as supplied from commercial sources with the following exceptions. Hexane, ethyl acetate, chloroform, dichloromethane, tetrahydrofuran, and triethylamine were distilled from calcium hydride immediately prior to use. Methanol was dried from magnesium methoxide as follows. Magnesium turnings (5 g) and iodine (0.5 g) were refluxed in a small (50–100 mL) quantity of methanol until all of the magnesium has reacted. The mixture was diluted (up to 1 L) with reagent grade methanol, refluxed for 2–3 h, and then distilled under nitrogen. All reactions were carried out under argon atmosphere using flame-dried glassware.

The purities of compounds were determined to be greater than 95% by HPLC. Compound **23** was prepared as previously reported.[7]

Synthesis

Alcohol **24**. 2,6-lutidine (20 eq.) and tert-butyldimethylsilyl trifluoromethanesulfonate (6 eq.) were added at 0°C to a solution of compound **23** (1.5 g, 3.9 mmol) in 20 mL of CH_2Cl_2. After 2 h stirring at 0°C, the reaction was quenched by addition of aqueous $NaHSO_4$ (1M, 100 mL). The layers were separated, and the aqueous phase was extracted with CH_2Cl_2 (3 × 50 mL). The combined organic layers were washed with $NaHSO_4$ 1M, water, saturated aqueous $NaHCO_3$, and brine and evaporated in vacuo to give 2.8 g of methyl 3β-tertbutyldimethylsilyloxy-5-en-24-oate in the form of colorless needles, that was subjected to next step without any purification. To a solution of methyl ester (5.7 mmol) in dry THF (30 mL), at 0°C dry methanol (7 eq.) and $LiBH_4$ (2M in THF, 7 eq.) were added. The resulting mixture was stirred for 2 h at 0°C. The mixture was quenched by addition of 1M NaOH (11.4 mL) and then ethyl acetate. The organic phase was washed with water, dried on Na_2SO_4 and concentrated. Purification by silica gel (hexane/ethyl acetate 9:1 v/v and 0.5% TEA) gave compound **24** as a white solid (1.5 g, 82% over two steps).

Mitsunobu reaction. In seven different aliquots DIAD (3.5 eq) was added dropwise to a solution of PPh_3 (3.5 eq) in dry THF at 0 °C. The suspension was stirred for 10 min, then a solution of compound **24** (1.5 g, 3.2 mmol) in dry THF was added. After 10 min, a solution of the corresponding phenols (methyl 4-hydroxybenzoate, 4-(trifluoromethyl)phenol, 4-hydroxybenzonitrile, methyl 3-hydroxybenzoate, 3-(trifluoromethyl)phenol, 3-hydroxybenzonitrile, and methyl 3,5-dihydroxybenzoate, respectively) in dry THF was added. After a period of 3h-overnight, water (10 mL) was added and the reaction mixture was evaporated at rotavapor. The residue was than extracted with EtOAc (3 x 50 mL). The combined organic layers were washed with a solution of KOH 2.5 M and water, dried and evaporated to give a yellow oil, which was subjected to deprotection without purification. The crude product was solubilized in dry THF and then an excess of tetra-*n*-butylammonium fluoride (TBAF) solution (1M in THF dry) was added. When the reaction was completed, it was extracted for three times with H_2O and EtOAc (3 x 30 mL). Then the organic layer was dried, filtered and concentrated under vacuum to give a crude residue. Purification by flash chromatography gave compounds **1, 4, 5, 6, 9**, **10**, and **11**.

24-(4-(methoxycarbonyl)phenoxy)-5-cholen-3β-ol (1). Purification by flash chromatography on silica gel with DCM 100% as eluent gave compound **1** (57%). Selected ^{1}H NMR ($CDCl_3$, 400 MHz): δ 7.98 (2H, d, *J* = 8.6 Hz, H-3',5'), 6.89 (2H, d, *J* = 8.6 Hz, H-2',6'), 5.32 (1H, br s, H-6), 3.97 (2H, m, H_2-24), 3.88 (3H, s, OCH_3), 3.49 (1H, m, H-3α), 1.00 (3H, s, Me-19), 0.97 (3H, d, *J* = 6.5 Hz, Me-21), 0.69 (3H, s, Me-18). ^{13}C NMR ($CDCl_3$, 100 MHz) δ 166.8, 162.9, 140.7, 131.5 (2C), 122.3, 121.6, 114.0 (2C), 71.7, 68.7, 56.7, 55.9, 51.8, 50.1, 42.3, 42.2, 39.8, 37.2, 36.4, 35.4, 32.0, 31.9 (2C), 31.6, 28.2, 25.7, 24.2, 21.0, 19.4, 18.6, 11.8. HPLC purity: >95%. HRMS-ESI calculated for $C_{32}H_{47}O_4^+$ $[M + H]^+$: 495.3469. Found: 495.3465.

24-(4-(trifluoromethyl)phenoxy)-5-cholen-3β-ol (4). Purification by flash chromatography on silica gel (dichloromethane 100%) gave compound **4** (55%). Selected ^{1}H NMR ($CDCl_3$, 400 MHz): δ 7.53 (2H, d, *J* = 8.2 Hz, H-3',5'), 6.94 (2H, d, *J* = 8.2 Hz, H-2',6'), 5.36 (1H, br s, H-6), 3.97 (2H, br s, H_2-24), 3.53 (1H, m, H-3α), 1.02 (3H, s, Me-19), 0.98 (3H, d, *J* = 6.3 Hz, Me-21), 0.70 (3H, s, Me-18). ^{13}C NMR ($CDCl_3$, 100 MHz) δ 161.5, 140.8, 126.8 (2C), 124.1, 121.6, 121.3, 114.2 (2C), 71.7, 68.7, 56.7, 55.9, 50.1, 42.3, 42.2, 39.7, 37.2, 36.5, 35.5, 32.0, 31.9 (2C), 31.6, 28.2, 25.7, 24.2, 21.1, 19.4, 18.6, 11.9. HPLC purity: >95%. HRMS-ESI calculated for $C_{31}H_{44}F_3O_2^+$ $[M + H]^+$: 505.3288. Found: 505.3286.

24-(4-cyanophenoxy)-5-cholen-3β-ol (5). Purification by flash chromatography on silica gel (DCM 100%) gave pure compound **5** (1.26 mmol, quantitative yield). Selected ^{1}H NMR ($CDCl_3$, 400 MHz): δ 7.57 (2H, d, *J* = 8.7 Hz, H-3',5'), 6.93 (2H, d, *J* = 8.7 Hz, H-2',6'), 5.35 (1H, d, *J* = 4.4 Hz, H-6), 3.97 (2H, dd, *J* = 9.4, 6.4 Hz, H_2-24), 3.52 (1H, m, H-3α), 1.01 (3H, s, Me-19), 0.97 (3H, d, *J* = 6.5 Hz, Me-21), 0.69 (3H, s, Me-18). ^{13}C NMR ($CDCl_3$, 100 MHz) δ 162.4, 140.7, 133.9 (2C), 121.7, 121.6, 115.1 (2C), 103.6, 71.7, 68.8, 56.7, 55.8, 50.0, 42.3, 42.2, 39.7, 37.2, 36.5, 35.4, 31.9, 31.8 (2C), 31.6, 28.2, 25.6, 24.2, 21.0, 19.3, 18.6, 11.9. HPLC purity: >95%. HRMS-ESI calculated for $C_{31}H_{44}NO_2^+$ $[M + H]^+$: 462.3367. Found: 462.3365.

24-(3-(methoxycarbonyl)phenoxy)-5-cholen-3β-ol (6). Purification by flash chromatography on silica gel with DCM 100% as eluent gave compound **6** (62%). Selected ^{1}H NMR ($CDCl_3$, 500 MHz):

δ 7.62 (1H, d, *J* = 7.9 Hz, H-4'), 7.55 (1 H, br s, H-2'), 7.33 (1H, t, *J* = 7.9 Hz, H-5'), 7.09 (1H, dd, *J* = 7.9, 1.7 Hz, H-6'), 5.36 (1H, d, *J* = 5.0 Hz, H-6), 3.98 (2H, dd, *J* = 11.7, 6.4 Hz, H_2-24), 3.53 (1H, m, H-3α), 1.02 (3H, s, Me-19), 0.98 (3H, d, *J* = 6.6 Hz, Me-21), 0.70 (3H, s, Me-18). ^{13}C NMR ($CDCl_3$, 100 MHz) δ 167.0, 159.1, 140.8, 131.3, 129.3, 121.8, 121.7, 119.9, 114.7, 71.8, 68.7, 56.7, 55.9, 52.1, 50.1, 42.4, 42.3, 39.8, 37.2, 36.5, 35.5, 32.0, 31.9 (2C), 31.6, 28.2, 25.8, 24.3, 21.0, 19.4, 18.6, 11.9. HPLC purity: >95%. HRMS-ESI calculated for $C_{32}H_{47}O_4^+$ $[M + H]^+$: 495.3469. Found: 495.3471.

24-(3-(trifluoromethyl)phenoxy)-5-cholen-3β-ol (9). Purification by flash chromatography on silica gel (DCM 100%) gave compound **9** (87%). Selected ^{1}H NMR ($CDCl_3$, 400 MHz): δ 7.37 (1H, t, *J* = 8.2 Hz, H-5'), 7.19 (1H, d, *J* = 7.5 Hz, H-4'), 7.12 (1H, s, H-2'), 7.06 (1H, d, *J* = 8.2 Hz, H-6'), 5.36 (1H, br s, H-6), 3.96 (2H, m, H_2-24), 3.53 (1H, m, H-3α), 1.02 (3H, s, Me-19), 0.98 (3H, d, *J* = 6.4 Hz, Me-21), 0.70 (3H, s, Me-18). ^{13}C NMR ($CDCl_3$, 100 MHz) δ 159.2, 140.7, 131.3, 129.8, 124.4, 121.6, 117.9, 117.1, 111.2, 71.7, 68.7, 56.7, 55.9, 50.1, 42.3, 42.2, 39.7, 37.2, 36.4, 35.5, 32.0, 31.9 (2C), 31.6, 28.2, 25.7, 24.2, 21.0, 19.3, 18.6, 11.8. HPLC purity: >95%. HRMS-ESI calculated for $C_{31}H_{44}F_3O_2^+$ $[M + H]^+$: 505.3288. Found: 505.3287.

24-(3-cyanophenoxy)- 5-cholen-3β-ol (10). Purification by flash chromatography on silica gel (DCM 100%) gave compound **10** (36%). Selected ^{1}H NMR ($CDCl_3$, 400 MHz): δ 7.36 (1H, m, H-5'), 7.23 (1H, d, *J* = 7.5 Hz, H-4'), 7.13 (1 H, s, H-2'), 7.12 (1H, ovl, H-6'), 5.36 (1H, d, *J* = 3.8 Hz, H-6), 3.94 (2H, m, H_2-24), 3.53 (1H, m, H-3α), 1.02 (3H, s, Me-19), 0.98 (3H, d, *J* = 6.5 Hz, Me-21), 0.70 (3H, s, Me-18). ^{13}C NMR ($CDCl_3$, 100 MHz) δ 159.2, 140.7, 130.2, 124.2, 121.6, 119.8, 118.8, 117.4, 113.2, 71.8, 68.9, 56.7, 55.9, 50.1, 42.4, 42.3, 39.8, 37.3, 36.5, 35.5, 32.0, 31.9 (2C), 31.6, 28.2, 25.6, 24.2, 21.1, 19.4, 18.6, 11.9. HPLC purity: >95%. HRMS-ESI calculated for $C_{31}H_{44}NO_2^+$ $[M + H]^+$: 462.3367. Found: 462.3364.

24-(3-hydroxy-5-(methoxycarbonyl)phenoxy)-5-cholen-3β-ol (11). Purification by flash chromatography on silica gel (DCM 100%) gave compound **11** (quantitative yield). An analytical sample was purified by HPLC on a Phenomenex Luna C18 PFP column (5 μm; 4.6 mm i.d. x 250

mm), with MeOH/H_2O (85:15) as eluent (flow rate 1 mL/min) (t_R = 15.6 min) furnishing a pure amount of compound **11**. Selected ^1H NMR ($CDCl_3$, 400 MHz): δ 7.15 (1H, br s, H-6'), 7.10 (1H, br s, H-4'), 6.60 (1H, t, *J* = 2.4 Hz, H-2'), 5.36 (1H, d, *J* = 5.2 Hz, H-6), 3.95 (2H, m, H_2-24), 3.91 (3H, s, OCH_3), 3.54 (1H, m, H-3α), 1.02 (3H, s, Me-19), 0.98 (3H, d, *J* = 6.5 Hz, Me-21), 0.70 (3H, s, Me-18). ^{13}C NMR ($CDCl_3$, 100 MHz): δ 166.8, 160.4, 156.7, 140.7, 132.1, 121.7, 108.9, 107.9, 106.9, 71.8, 68.9, 56.8, 55.9, 52.3, 50.0, 42.3, 42.2, 39.8, 37.2, 36.5, 35.5, 32.0, 31.9 (2C), 31.7, 28.2, 25.8, 24.3, 21.1, 19.4, 18.7, 11.9. HPLC purity: >95%. HRMS-ESI calculated for $C_{32}H_{47}O_5^+$ $[M + H]^+$: 511.3418. Found: 511.3421.

$LiBH_4$ reduction. Esters **1** (0.33 mmol), **6** (0.55 mmol), and **11** (0.30 mmol) were subjected to $LiBH_4$ reduction, in the same conditions previously described, to give derivatives **2**, **7** and **12** as crude residues, in quantitative yields. Then the crudes were subjected to purification through flash chromatography or HPLC.

24-(4-(hydroxymethyl)phenoxy)-5-cholen-3β-ol (2). The crude obtained from $LiBH_4$ reduction (0.0347 mmol, quantitative yield) was purified by HPLC on a Phenomenex Luna C18 column (5 μm; 4.6 mm i.d. x 250 mm), with MeOH/H_2O (88:12) as eluent (flow rate 1 mL/min) (t_R = 20.0 min) furnishing an analytic sample of compound **2**. Selected ^1H NMR ($CDCl_3$, 500 MHz): δ 7.29 (2H, d, *J* = 8.3 Hz, H-3',5'), 6.89 (2H, d, *J* = 8.3 Hz, H-2',6'), 5.37 (1H, br s, H-6), 4.63 (2H, d, *J* = 5.8 Hz, CH_2OH), 3.93 (2H, dd, *J* = 11.9, 6.3 Hz, H_2-24), 3.53 (1H, m, H-3α), 1.02 (3H, s, Me-19), 0.98 (3H, d, *J* = 6.4 Hz, Me-21), 0.70 (3H, s, Me-18). ^{13}C NMR ($CDCl_3$, 100 MHz) δ 158.8, 140.7, 132.9, 128.6 (2C), 121.7, 114.6 (2C), 71.8, 68.6, 65.1, 56.7, 55.9, 50.1, 42.3, 42.2, 39.7, 37.2, 36.5, 35.5, 32.1, 31.9 (2C), 31.6, 28.2, 25.8, 24.3, 21.0, 19.4, 18.6, 11.9. HPLC purity: >95%. HRMS-ESI calculated for $C_{31}H_{47}O_3^+$ $[M + H]^+$: 467.3520. Found: 467.3524.

24-(3-(hydroxymethyl)phenoxy)-5-cholen-3β-ol (7). Purification by flash chromatography on silica gel (DCM 100%) gave compound **7** (38%). An analytic sample was obtained by HPLC on a Phenomenex Luna C18 column (5 μm; 4.6 mm i.d. x 250 mm), with MeOH/H_2O (92:8) as eluent (flow rate 1 mL/min) (t_R = 12.0 min). Selected ^1H NMR ($CDCl_3$, 400 MHz): δ 7.27 (1H, ovl, H-5'),

6.93 (1 H, ovl, H-2'), 6.92 (1H, ovl, H-4'), 6.83 (1H, dd, *J* = 8.3, 1.9 Hz, H-6'), 5.36 (1H, d, *J* = 5.0 Hz, H-6), 4.68 (2H, s, CH_2OH), 3.94 (2H, m, H_2-24), 3.53 (1H, m, H-3α), 1.02 (3H, s, Me-19), 0.98 (3H, d, *J* = 6.5 Hz, Me-21), 0.70 (3H, s, Me-18). ^{13}C NMR ($CDCl_3$, 100 MHz) δ 159.4, 142.4, 140.7, 129.6, 121.7, 118.9, 113.8, 112.9, 71.8, 68.5, 65.4, 56.7, 55.9, 50.1, 42.3, 42.2, 39.8, 37.2, 36.5, 35.5, 32.1, 31.9 (2C), 31.6, 28.2, 25.9, 24.3, 21.0, 19.4, 18.6, 11.9. HPLC purity: >95%. HRMS-ESI calculated for $C_{31}H_{47}O_3^+$ $[M + H]^+$: 467.3520. Found: 467.3525.

24-(3-hydroxy-5-(hydroxymethyl)phenoxy)-5-cholen-3β-ol (12). Purification by flash chromatography on silica gel (DCM 100%) gave compound **12** (86%). An analytic sample was obtained by HPLC on a Phenomenex Luna C18 PFP column (5 μm; 4.6 mm i.d. x 250 mm), with MeOH/H_2O (85:15) as eluent (flow rate 1 mL/min) (t_R = 8.0 min). Selected ^1H NMR ($CDCl_3$, 400 MHz): δ 6.51 (1H, s, H-6'), 6.44 (1H, s, H-2'), 6.33 (1H, s, H-4'), 5.36 (1H, d, *J* = 5.3 Hz, H-6), 4.61 (2H, s, CH_2OH), 3.91 (2H, m, H_2-24), 3.53 (1H, m, H-3α), 1.02 (3H, s, Me-19), 0.95 (3H, d, *J* = 6.6 Hz, Me-21), 0.71 (3H, s, Me-18). ^{13}C NMR ($CDCl_3$, 100 MHz): δ 160.5, 156.9, 143.4, 140.8, 121.6, 105.7, 105.4, 101.1, 71.8, 68.7, 65.2, 56.8, 56.1, 50.1, 42.3, 42.2, 39.7, 37.3, 36.5, 35.6, 32.0, 31.9 (2C), 31.7, 28.3, 25.1, 24.3, 21.0, 19.4, 18.7, 11.9. HPLC purity: >95%. HRMS-ESI calculated for $C_{31}H_{47}O_4^+$ $[M + H]^+$: 483.3469. Found: 483.3466.

Basic hydrolysis. Another three aliquots of compounds **1** (0.33 mmol), **6** (0.22 mmol), and **11** (0.30 mmol) were hydrolyzed with NaOH pellets (10 eq.) in a solution of MeOH: H_2O 1:1 v/v (20 mL) at reflux. When the reactions were completed, the resulting solutions were concentrated under vacuum, diluted with water, acidified with HCl 6 N and extracted with ethyl acetate (3 x 50 mL). The collected organic phases were washed with brine, dried over Na_2SO_4 anhydrous, and evaporated under reduced pressure to furnish carboxylic acids **3**, **8** and **13** as crude residues, in quantitative yields, that were subjected to purification through flash chromatography or HPLC.

24-(4-carboxyphenoxy)-5-cholen-3β-ol (3). The crude obtained from NaOH hydrolysis (0.0434 mmol, quantitative yield) was then purified by HPLC on a Phenomenex Luna C18 (5 μm; 4.6 mm i.d. x 250 mm), with MeOH/H_2O (90:10) (flow rate 1 mL/min) (t_R = 19.5 min) giving a pure sample

of compound **3**. Selected ^{1}H NMR ($CDCl_3$, 400 MHz): δ 8.03 (2H, d, *J* = 8.3 Hz, H-3',5'), 6.93 (2H, d, *J* = 8.3 Hz, H-2',6'), 5.36 (1H, d, *J* = 4.0 Hz, H-6), 4.00 (2H, m, H_2-24), 3.53 (1H, m, H-3α), 1.02 (3H, s, Me-19), 0.98 (3H, d, *J* = 6.4 Hz, Me-21), 0.70 (3H, s, Me-18).^{13}C NMR ($CDCl_3$, 100 MHz) δ 166.8, 163.5, 140.7, 132.1 (2C), 121.6, 121.3, 114.2 (2C), 71.8, 68.8, 56.8, 55.9, 50.1, 42.3, 42.2, 39.8, 37.2, 36.5, 35.5, 32.0, 31.9 (2C), 31.6, 28.2, 25.7, 24.3, 21.1, 19.4, 18.7, 11.9. HPLC purity: >95%. HRMS-ESI calculated for $C_{31}H_{43}O_4^-$ [M - H]$^-$: 479.3166. Found: 479.3163.

24-(3-carboxyphenoxy)-5-cholen-3β-ol (8). Purification by flash chromatography on silica gel (DCM:MeOH 9:1 v/v) gave compound **8** (24.3%). An analytic sample was obtained by HPLC on a Phenomenex Luna C18 column (5 μm; 4.6 mm i.d. x 250 mm), with MeOH/H_2O (88:12) as eluent (flow rate 1 mL/min) (t_R =25 min). Selected ^{1}H NMR ($CDCl_3$, 400 MHz): δ 7.68 (1H, d, *J* = 7.9 Hz, H-4'), 7.59 (1 H, s, H-2'), 7.37 (1H, t, *J* = 7.9 Hz, H-5'), 7.14 (1H, dd, *J* = 7.9, 3.9 Hz, H-6'), 5.36 (1H, br s, H-6), 3.99 (2H, m, H_2-24), 3.54 (1H, m, H-3α), 1.02 (3H, s, Me-19), 0.98 (3H, d, *J* = 6.4 Hz, Me-21), 0.70 (3H, s, Me-18). ^{13}C NMR ($CDCl_3$, 100 MHz) δ 167.4, 159.4, 140.7, 129.9, 122.7, 122.0, 121.1, 120.7, 115.4, 72.1, 69.0, 56.4, 55.9, 50.2, 42.5, 42.2, 40.0, 37.5, 36.6, 35.8, 32.3, 32.1, 31.8, 31.4, 28.5, 26.0, 24.4, 21.2, 19.6, 18.8, 12.1. HPLC purity: >95%. HRMS-ESI calculated for $C_{31}H_{43}O_4^-$ [M - H]$^-$: 479.3166. Found: 479.3167.

24-(3-carboxy-5-hydroxyphenoxy)-5-cholen-3β-ol (13). Purification by flash chromatography on silica gel (DCM 100%) gave compound **13** (79%). An analytic sample was obtained by HPLC on a Phenomenex Luna C18 PFP column (5 μm; 4.6 mm i.d. x 250 mm), with MeOH/H_2O (80:20) and 0.1% TFA as eluent (flow rate 1 mL/min) (t_R = 16.4 min). Selected ^{1}H NMR (CD_3OD, 400 MHz): δ 7.03 (2H, s, H-4'-H-6'), 6.55 (1H, s, H-2'), 5.34 (1H, d, *J* = 5.0 Hz, H-6), 4.61 (2H, s, CH_2OH), 3.91 (2H, t, *J* = 6.4 Hz, H_2-24), 3.40 (1H, m, H-3α), 1.02 (3H, s, Me-19), 1.00 (3H, d, *J* = 6.6 Hz, Me-21), 0.73 (3H, s, Me-18). ^{13}C NMR (CD_3OD, 100 MHz): δ 169.9, 159.7, 145.9, 142.3, 135.4, 122.5, 110.1, 107.7, 107.5, 72.4, 69.6, 58.2, 57.4, 51.7, 43.5, 43.0, 41.1, 38.5, 37.7, 36.8, 33.3, 33.2, 33.0, 32.3, 29.3, 26.9, 25.3, 22.2, 19.9, 19.2, 12.3. HPLC purity: >95%. HRMS-ESI calculated for $C_{31}H_{43}O_5^-$ [M - H]$^-$: 495.3116. Found: 495.3112.

Compound 25. To a solution of Lithocholic acid (LCA) (1.0 g, 2.67 mmol) in dry MeOH (50 mL), *p*-toluensulfonic acid was added (4 eq.) at room temperature. After 1h, the reaction was quenched through the addition of $NaHCO_3$ saturated solution until neutralization. Then, the solvent was removed under vacuum and the residue was extracted with H_2O/EtOAc (3 x 100 mL). The combined organic layers were washed with $NaHCO_3$ saturated solution and then with water, dried on Na_2SO_4 and evaporated to give the corresponding LCA methyl ester (4.0 mmol) in quantitative yied. This intermediate was then solubilized in dry DCM (50 mL). At the solution were added 2,6-lutidine (7 eq.) and tert-butyldimethylsilyl trifluoromethanesulfonate (1.5 eq.) at 0°C. After 2h, the reaction was quenched by addition of $NaHSO_4$ solution (1M, 100 mL) and then extracted with DCM (3 x 100 mL). The combined organic layers were washed with $NaHSO_4$ 1M, $NaHCO_3$ saturated solution and water, dried, filtered and concentrated to furnish compound **25** (5.0 mmol) in quantitative yield, which was subjected to the next step without purification.

Compound 26. The title compound was prepared according to the procedure described for $LiBH_4$ reduction. Purification on silica gel (Hexane/EtOAC 9:1 + 0.5% TEA) furnished a pure alcohol **26** (3.35 mmol, 67% yield).

Mitsunobu reaction. Four different aliquots of alcohol **26** (0.840 mmol) were subjected to Mitsunobu reaction, performed in the same synthetic conditions described before. Purification on silica gel with Hexane 100% + 0.5% TEA furnished pure protected intermediates which were subjected to deprotection with an excess of TBAF 1M solution. An additional purification by flash chromatography gave compounds **14**, **17**, **18** and **21** (50-70% yields).

24-(4-(methoxycarbonyl)phenoxy)-5β-cholan-3α-ol (14). Purification by flash chromatography on silica gel (99.5:0.5 hexane/AcOEt) gave compound **14** (64%). An analytic sample was obtained by HPLC on a semipreparative Macherey-Nagel C18 column (10 μm; 4.6 mm i.d. x 250 mm), with MeOH/H_2O (95:5) as eluent (flow rate 3 mL/min) (t_R = 41.0 min). Selected ^{1}H NMR ($CDCl_3$, 400 MHz): δ 7.98 (2H, d, *J* = 8.7 Hz, H-3',5'), 6.90 (2H, d, *J* = 8.7 Hz, H-2',6'), 3.98 (2H, m, H_2-24), 3.88 (3H, s, OCH_3), 3.62 (1H, m, H-3α), 0.95 (3H, d, *J* = 6.6 Hz, Me-21), 0.92 (3H, s, Me-19), 0.65

(3H, s, Me-18). ^{13}C NMR ($CDCl_3$, 100 MHz): δ 167.0, 162.9, 131.6(2C), 122.3, 114.1(2C), 71.9, 68.7, 56.5, 56.1, 51.9, 42.7, 42.1, 40.4, 40.2, 36.4, 35.8, 35.5, 35.3, 34.6, 32.0, 30.5, 28.3, 27.2, 26.4, 25.8, 24.2, 23.4, 20.8, 18.6, 12.1. HPLC purity: >95%. HRMS-ESI calculated for $C_{32}H_{49}O_4^+$ [M + H]$^+$: 497.3625. Found: 497.3623.

24-(4-cyanophenoxy)-5β-cholan-3α-ol (17). Purification by flash chromatography on silica gel (99.5:0.5 hexane/AcOEt) gave compound **17** (quantitative yield). Selected ^{1}H NMR ($CDCl_3$, 400 MHz):δ 7.56 (2H, d, *J* = 8.5 Hz, H-3',5'), 6.92 (2H, d, *J* = 8.5 Hz, H-2',6'), 3.96 (2H, m, H_2-24), 3.62 (1H, m, H-3α), 0.95 (3H, d, *J* = 6.6 Hz, Me-21), 0.92 (3H, s, Me-19), 0.65 (3H, s, Me-18). ^{13}C NMR ($CDCl_3$, 100 MHz): δ 162.5, 133.9 (2C), 119.3, 115.2 (2C), 103.6, 71.7, 68.9, 56.4, 56.0, 42.6, 42.0, 40.4, 40.1, 36.3, 35.8, 35.4, 35.3, 34.5, 31.9, 30.4, 28.3, 27.2, 26.4, 25.6, 24.1, 23.3, 20.7, 18.5, 12.0. HPLC purity: >95%. HRMS-ESI calculated for $C_{31}H_{46}NO_2^+$ [M + H]$^+$: 464.3523. Found: 464.3525.

24-(3-(methoxycarbonyl)phenoxy)-5β-cholan-3α-ol (18). Purification by flash chromatography on silica gel (99.5:0.5 hexane/AcOEt) gave compound **18** (24%). An analytic sample was obtained by HPLC on a semipreparative Macherey-Nagel C18 column (10 μm; 4.6 mm i.d. x 250 mm), with MeOH/H_2O (95:5) as eluent (flow rate 3 mL/min) (t_R = 24.0 min) gave compound **18**. Selected ^{1}H NMR ($CDCl_3$, 400 MHz): δ 7.61 (1H, d, *J* = 8.0 Hz, H-4'), 7.55 (1H, s, H-2'), 7.33 (1H, t, *J* = 8.0 Hz, H-5'), 7.09 (1H, d, *J* = 8.0 Hz, H-6'), 3.98 (2H, m, H_2-24), 3.91 (3H, s, OCH_3), 3.62 (1H, m, H-3α), 0.95 (3H, d, *J* = 6.6 Hz, Me-21), 0.92 (3H, s, Me-19), 0.65 (3H, s, Me-18). ^{13}C NMR ($CDCl_3$, 100 MHz): δ 167.1, 162.9, 130.4, 129.6, 119.8, 118.7, 114.1, 71.9, 68.8, 56.5, 56.0, 51.9, 42.7, 42.1, 40.4, 40.2, 36.4, 35.7, 35.5, 35.3, 34.5, 31.9, 30.5, 28.3, 27.2, 26.4, 25.7, 24.2, 23.4, 20.8, 18.6, 12.1. HPLC purity: >95%. HRMS-ESI calculated for $C_{32}H_{49}O_4^+$ [M + H]$^+$: 497.3625. Found: 497.3621.

24-(3-cyanophenoxy)-5β-cholan-3α-ol (21). Purification by flash chromatography on silica gel (99:1 dichloromethane/MeOH) gave compound **21** (quantitative yield). Selected ^{1}H NMR ($CDCl_3$, 400 MHz): δ 7.35 (1H, t, *J* = 7.7 Hz, H-5'), 7.26 (1H, s, H-2'), 7.21 (1H, d, *J* = 7.7 Hz, H-4'), 7.11 (1H, d, *J* = 7.7 Hz, H-6'), 3.98 (2H, m, H_2-24), 3.62 (1H, m, H-3α), 0.95 (3H, d, *J* = 6.6 Hz, Me-

21), 0.92 (3H, s, Me-19), 0.65 (3H, s, Me-18). ^{13}C NMR ($CDCl_3$, 100 MHz): δ 159.2, 130.2, 124.2, 119.8, 118.7, 117.4, 113.1, 71.8, 68.9, 56.5, 56.0, 42.7, 42.1, 40.4, 40.2, 36.4, 35.8, 35.5, 35.3, 34.5, 31.9, 30.5, 28.3, 27.2, 26.4, 25.7, 24.2, 23.4, 20.8, 18.6, 12.1. HPLC purity: >95%. HRMS-ESI calculated for $C_{31}H_{46}NO_2^+$ $[M + H]^+$: 464.3523. Found: 464.3522.

Synthesis of compounds 15 and 18. Esters **14** (0.17 mmol) and **18** (0.06 mmol) were subjected to $LiBH_4$ reduction, in the same conditions previously described, to give respectively derivatives **15** and **19** as crude residues, that were subjected to purification through flash chromatography or HPLC.

24-(4-(hydroxymethyl)phenoxy)-5β-cholan-3α-ol (15). The crude obtained from $LiBH_4$ reduction (92%) was purified by HPLC on a Macherey Nagel C18 column (5 μm; 10 mm i.d. x 250 mm), with MeOH/H_2O (92:8) as eluent (flow rate 3 mL/min) (t_R = 26.0 min) furnishing an analytic sample of compound **15**. Selected ^{1}H NMR ($CDCl_3$, 500 MHz): δ 7.28 (2H, d, *J* = 8.4 Hz, H-3',5'), 6.88 (2H, d, *J* = 8.4 Hz, H-2',6'), 4.62 (2H, d, *J* = 5.8 Hz, CH_2OH), 3.92 (2H, dd, *J* = 11.9, 6.3 Hz, H_2-24), 3.62 (1H, m, H-3α), 0.94 (3H, d, *J* = 6.4 Hz, Me-21), 0.91 (3H, s, Me-19), 0.64 (3H, s, Me-18). ^{13}C NMR ($CDCl_3$, 100 MHz): δ 158.8, 132.9, 128.6(2C), 114.6(2C), 71.9, 68.6, 65.2, 56.6, 56.1, 42.7, 42.1, 40.4, 40.2, 36.5, 35.9, 35.5, 35.3, 34.6, 32.1, 30.6, 28.3, 27.2, 26.5, 25.9, 24.1, 23.4, 20.9, 18.6, 12.1. HPLC purity: >95%. HRMS-ESI calculated for $C_{31}H_{49}O_3^+$ $[M + H]^+$: 469.3676. Found: 469.3673.

24-(3-(hydroxymethyl)phenoxy)-5β-cholan-3α-ol (19). The crude obtained from $LiBH_4$ reduction (86%) was purified by HPLC on a Phenomenex C18 PFP column (5 μm; 4.6 mm i.d. x 250 mm), with MeOH/H_2O (88:12) as eluent (flow rate 1 mL/min) (t_R = 10.0 min). Selected ^{1}H NMR ($CDCl_3$, 400 MHz): δ 7.27 (1H, ovl, H-5'), 6.92 (2H, ovl, H-2'and H-4'), 6.82 (1H, d, *J* = 8.1 Hz, H-6'), 4.67 (2H, s, CH_2OH), 3.93 (2H, m, H_2-24), 3.62 (1H, m, H-3α), 0.94 (3H, d, *J* = 6.5 Hz, Me-21), 0.91 (3H, s, Me-19), 0.64 (3H, s, Me-18). ^{13}C NMR ($CDCl_3$, 100 MHz): δ 158.1, 142.5, 129.6, 118.9, 113.9, 112.9, 71.9, 68.5, 65.4, 56.6, 56.2, 42.7, 42.1, 40.4, 40.2, 36.4, 35.8, 35.5, 35.4, 34.6, 32.1, 30.5, 28.3, 27.2, 26.5, 25.9, 24.3, 23.4, 20.8, 18.6, 12.1. HPLC purity: >95%. HRMS-ESI calculated for $C_{31}H_{49}O_3^+$ $[M + H]^+$: 469.3676. Found: 469.3674.

Synthesis of compounds 16 and 20. Another two aliquots of compounds **14** (0.108 mmol) and **18** (0.058 mmol) were hydrolyzed with NaOH pellets (10 eq.) with the same procedure described in Scheme 1 (step j), to furnish carboxylic acids **16** and **20** as crude residues, that were subjected to purification through flash chromatography or HPLC.

24-(4-carboxyphenoxy)-5β-cholan-3α-ol (16). The crude obtained from NaOH hydrolysis (89%) was then purified by HPLC on Macherey Nagel C18 column (5 μm; 10 mm i.d. x 250 mm), with MeOH/H_2O (97:3) as eluent (flow rate 3 mL/min) (t_R = 15.0 min) giving a pure sample of compound **16**. Selected ^{1}H NMR ($CDCl_3$, 400 MHz): δ 8.03 (2H, d, *J* = 8.7 Hz, H-3',5'), 6.92 (2H, d, *J* = 8.7 Hz, H-2',6'), 3.98 (2H, m, H_2-24), 3.63 (1H, m, H-3α), 0.95 (3H, d, *J* = 6.6 Hz, Me-21), 0.91 (3H, s, Me-19), 0.64 (3H, s, Me-18). ^{13}C NMR ($CDCl_3$, 100 MHz): δ 168.8, 160.9, 132.3 (2C), 121.9, 114.2 (2C), 71.9, 68.8, 56.5, 56.1, 42.7, 42.1, 40.5, 40.2, 36.4, 35.8, 35.5, 35.3, 34.6, 32.0, 30.5, 28.3, 27.2, 26.4, 25.7, 24.2, 23.4, 20.9, 18.6, 12.1. HPLC purity: >95%. HRMS-ESI calculated for $C_{31}H_{45}O_4^-$ [M - H]$^-$: 481.3323. Found: 481.3325.

24-(3-carboxyphenoxy)-5β-cholan-3α-ol (20). The crude obtained from NaOH hydrolysis (95%) was then purified by HPLC on Macherey Nagel C18 column (5 μm; 10 mm i.d. x 250 mm), with MeOH/H_2O (97:3) as eluent (flow rate 3 mL/min) (t_R = 16.0 min) giving a pure sample of compound **20.** Selected ^{1}H NMR ($CDCl_3$, 400 MHz): δ 7.66 (1H, d, *J* = 7.6 Hz, H-4'), 7.58 (1 H, s, H-2'), 7.36 (1H, t, *J* = 7.6 Hz, H-5'), 7.13 (1H, d, *J* = 7.6 Hz, H-6'), 3.98 (2H, m, H_2-24), 3.62 (1H, m, H-3α), 0.95 (3H, d, *J* = 6.6 Hz, Me-21), 0.92 (3H, s, Me-19), 0.65 (3H, s, Me-18). ^{13}C NMR ($CDCl_3$, 100 MHz): δ 169.5, 159.2, 130.4, 129.5, 122.5, 120.9, 115.2, 71.9, 68.8, 56.5, 56.0, 42.7, 42.1, 40.4, 40.2, 36.4, 35.8, 35.5, 35.4, 34.5, 32.0, 30.5, 28.3, 27.2, 26.4, 25.8, 24.3, 23.4, 20.8, 18.6, 12.1. HPLC purity: >95%. HRMS-ESI calculated for $C_{31}H_{45}O_4^-$ [M - H]$^-$: 481.3323. Found: 481.3322.

***In vitro* assays**

Luciferase reporter gene assay. To investigate the GPBAR1 activation, HEK-293T cells were transiently transfected with 200 ng of human pGL4.29 (Promega), a reporter vector containing a cAMP response element (CRE) that drives the transcription of the luciferase reporter gene luc2P,

with 100 ng of pCMVSPORT6-human GPBAR1 and with 100 ng of pGL4.70. At 24 h post-transfection, the cells were stimulated 18 h with 10 μM TLCA and some selected compounds (10 μM). After treatments, the cells were lysed in 100 μL of lysis buffer (25 mM tris-phosphate, pH 7.8; 2 mM dithiothreitol (DTT); 10% glycerol; 1% Triton X-100), and 10 μL of cellular lysate was assayed for luciferase activity using the luciferase assay system (Promega). Luminescence was measured using Glomax 20/20 luminometer (Promega). Luciferase activities were assayed and normalized with Renilla activities. The concentration-response curves were performed in HEK-293T cells transfected as described above and then treated with increasing concentrations of compounds **3**, **5**, **7** (from 0.1 to 50 μM). At 18 h post stimulations, cellular lysates were assayed for luciferase and Renilla activities using the Dual-Luciferase Reporter assay system (E1980, Promega). Luminescence was measured using a Glomax 20/20 luminometer (Promega). Luciferase activities were normalized with Renilla activities.

To investigate the FXR activation, HepG2 cells were transfected with 200 ng of the reporter vector p(hsp27)-TK-LUC containing the FXR response element IR1 cloned from the promoter of heat shock protein 27 (hsp27), 100 ng of pSG5-FXR, 100 ng of pSG5-RXR, and 100 of pGL4.70 (Promega), a vector encoding the human Renilla gene. At 24 h post transfection, cells were stimulated with compounds **3** and **7** (10 μM) and CDCA (**1**) were used as positive controls (Table S1).

To investigate the specificity of compounds **3** and **7** versus LXRα and LXRβ mediated transactivation, HepG2 cells were transfected with 200 ng of the reporter vector p(UAS)5XTKLuc, 100 ng of a vector containing the ligand binding domain of LXRα or LXRβ cloned upstream of the GAL4-DNA binding domain (i.e. pSG5-LXRαLBD-GAL4DBD or pSG5-LXRβLBD-GAL4DBD) and 100 of pGL4.70 (Promega), a vector encoding the human Renilla gene.

RORγ Human Assay. To evaluate inverse-agonist activities that compounds **3**, **5**, **7**,**15-17** and **19-21** exert against human RORγ, was used the "Human RORγ Reporter Assay System" kit (IB-IB04001, Indigo Biosciences). This nuclear receptor assay utilizes human cells engineered to provide high level expression of a hybrid form of the Human RAR-related Orphan Receptor Gamma. The N-terminal

DNA binding domains (DBD) of the native RORγ have been substituted with that of the yeast GAL4-DBD. As is true in vivo, these reporter cells express RORγ in a constant state of high-level activity. Briefly, 200 µl of Reporter Cells were dispensed into the wells of a 96 plate. After 4-6 h of pre-incubation, the growth medium was discarded and 200 µL of treatment medium (containing the compound from test) was added to each well. The compounds were tested at concentrations of 1 and 10 µM. In addition, a dose-response curve of an inverse reference agonist, ursolic acid (from 0.0165 to 6 µM) was performed, and untreated control wells were provided (100% activity). After 24 h of incubation, the treatment medium was discarded and 100 µL of Luciferase Detection Reagent was added. The reporter cells contain the cDNA encoding the enzyme Luciferase firefly (Photinus pyralis) downstream of the RORγ. The intensity of light emitted by each well was quantified using a plate reader for luminescence and was expressed in RLU (Relative Light Units).

Cofactor Peptide Recruitment Assay. The ability of synthetized compounds to interfere with the interaction between RORγ and SRC-1 or FXR and SRC-1 was evaluated employing AlphaScreen GST Detection Kit (PerkinElmer).

The experiments were conducted with 10 nM RORγ-LBD (aa 251-518, Creative Biomart) and 60 nM of biotinylated SRC-1 peptide (CPSSHSSLTERHKILHRLLQEGSPS) in the presence of 20 µg/mL donor and acceptor beads and in buffer containing 50 mM Tris-HCl (pH7.4), 20 mM KCl, 1 mM DTT, and 0.1% BSA. Incubations were performed in a final volume of 25 µL employing 384 wells Optiplate and measured by Envision 2105. For normalization of the data in Table 1, compounds were tested at 10 µM final concentration and the wells containing DMSO were defined as 100% control and the wells without the RORγt protein were defined as 0% control. To determine IC_{50} growing concentration of compounds were employed and data were analysed using Prism 7.

Activation of FXR has been measured by Alpha Screen Technology in a Coactivator Recruitment Assay employing 10nM GST-fusion FXR-LBD, and 30 nM biotinylated-SRC-1 peptide.

Solubility and LogD Measurements. Ten microliters of a 10 mM solution of each compound (**3** and **7**) were diluted either in 490 µL of PBS pH 7.4 or MeOH and shacked at 250 rpm for 24h at rt. Tubes were subsequently centrifuged for 5 min at 4000 rpm and 10 µL of each sample were further diluted in 490 µL of MeOH and analysed by LC-MS. The ratio of mass signal area obtained in PBS and in organic solvent was then calculated and used to determine solubility of each compound.

For LogD measurement, 40 µL of each compound were diluted in 1960 µL of PBS pH 7.4/Octanol and the mixtures were shacked for 2 h at rt. Then, organic and aqueous phases were separated, and after opportune dilution, each phase was analysed by LC-MS. LogD was calculated as the logarithm of the ratio of compounds concentrations in octanol and PBS.

Metabolic Stability. Compounds were tested in a buffer containing 50 mM potassium phosphate buffer (pH 7.4), 5 mM $MgCl_2$ and 1% DMSO, as vehicle. The final concentration of tested molecules was 1 µM and 0.5 mL the final volume of incubation. All incubations were performed under shaking at 37 °C and aliquots were removed at several time points after metabolizing fractions addition (0-240 min). For microsomes stability evaluation, the incubation mixtures contained 0.15 mg of human liver microsomes (Sigma-Aldrich, St. Louis, MO, USA) 1 mM NADPH, 5 mM glucose 6-phosphate, 0.4 $U \cdot mL^{-1}$ glucose 6-phosphate dehydrogenase whereas for S9 fraction analysis, 0.15 mg of S9 proteins were employed (Sigma-Aldrich, St. Louis, MO, USA), and the following cofactors were added to the mixtures: 1 mM NADP, 5 mM glucose-6-phosphate, 0.6 units/ml glucose-6-phosphate dehydrogenase, 0.4 mM UDP-glucuronic acid, 0.4 CoA, 0.1 mM 3'-phosphoadenosine 5'-phosphosulfate, 5 mM glutathione, 5 mM glycine, and 5 mM taurine. In both experiments, withdrawn aliquots were mixed with 200 µL of ice-cold acetonitrile to stop enzymatic activity. After two hours, samples were centrifuged for 10 min at 10,000 rpm, and supernatants were subjected to LC-MS analysis.

The slope of the linear regression of the curve obtained reporting the natural logarithm of compound area versus incubation time (−k) was used in the conversion to in vitro $t_{1/2}$ values by $t_{1/2} = -\ln(2)/k$.

In vitro intrinsic clearance (Clint expressed as μL/min/mg) was calculated according to the following formula: Clint = Vx 0.693/t1/2 were V = volume of reaction (μL)/protein in the incubation (mg). Testosterone was used as a positive control for microsome and phase I enzymes, and 7-hydroxycoumarin was used as positive control for phase II enzymes.

***In vitro* U937 cells assay.** U937 cells, a monocyte cell line were cultured at 37 °C in RPMI supplemented with 10% FBS, 1% glutamine, and 1% penicillin/streptomycin. In two different experimental sets, U937 were serum starved for 24 h and then were primed with LPS (100 ng/ml) and TNFα (100 ng/ml) alone or in combination with compounds **3** and **7** (0.1, 1, 10, 100 and 1000 nM) for another 24 h. At the end of the incubation, the cells were collected and resuspended in TRIzol reagent for RNA extraction with Direct-zol RNA MiniPrep (Zymo Research, USA) and for the following gene expression analysis.

Computational studies.

A docking and MD simulation protocol, that are widely employed to study ligand/protein binding interactions.[8–11] has been used to define the binding mode of the selected compounds in GPBAR1 and RORγ as follow:

Receptors and ligands preparation.

RORγ. The crystal structure of the human Retinoic acid receptor-related orphan receptor gamma (RORγ) (PDB ID 3l0j)[1] was downloaded from the Protein Data Bank website. The Nuclear receptor coactivator 2 (Src-2) in the RORγ active conformation, the co-crystallized ligands and water molecules were removed. Residues protonation states were assigned in accordance with the most populated ones predicted by the H++ webserver at pH 7.4.

GPBAR1. GPBAR1 homology model reported in D'Amore *et al.*[4] was employed for docking calculations. The receptor was prepared as reported in Biagioli *et al*[12]

Both the receptors were treated with the Protein Preparation Wizard Protein and ligand preparation: parameters, protocols, and influence on virtual screening enrichments [13] tool implemented in Maestro ver. 11.8.[14]

Ligands. The 3D structures of compounds **3** and **7** were built using the Graphical User Graphical User Interface (GUI) of Maestro ver. 11.8.[13] The protonation state of such compounds at pH 7.4 in water has been calculated using the Epik[14] module. Finally, **3** and **7** structures were minimized with the OPLS 2005 force field using the Polak-Ribiere Conjugate Gradient (PRCG) algorithm and 2500 iteration steps.[15]

Docking calculations. The docking procedure was carried out with the Glide software package,[16] using the Standard Precision (SP) algorithm of the GlideScore function[17,18] and the OPLS2005 force field,[19] since it showed to be the best protocol in reproducing the co-crystallized binding mode in the closed and active conformation of the RORγ receptor (PDB ID 3l0j)[1].

A grid box of 25 × 25 × 25 Å for RORγ receptor and one of 25 × 25 × 25 Å for GPBAR1 centered on the ligand binding cavity were created to compute the interaction grids. Default parameters were applied. A total amount of 100 poses was generated and the conformational sampling of the ligand was enhanced by two times, with respect to the default setting of Glide. Docking conformations of compounds **3** and **7** were then clustered based on their atomic RMSD with a threshold of 2Å. Globally, seven clusters were obtained and, among them, only the conformation included in the most populated cluster owing both the Glide Emodel and GlideScore lowest-energy value was considered.

Molecular dynamic simulation.

RORγ. Molecular dynamic simulations (MDs) were performed with NAMD ver. 2.12,[20] using the Amber *ff14SB* and the General Amber Force Field (GAFF) parameters[21,22] for the protein and the ligands, respectively. Each complex was solvated in a 10.0 Å layered cubic water box using the TIP3P water-model parameters (about 90000 atoms each). 89 Na^+ and 89 Cl^- ions were added to reproduce the experimental buffer conditions of 200 mM. The obtained system was thus subjected to three minimization steps using the conjugate gradient algorithm in the following conditions: *i)* energy minimization of water molecules and ions, keeping the solute restrained (50000 steps); *ii)* energy minimization of the system, keeping the protein backbone and ligand's atoms restrained (50000 steps); iii) energy minimization of the entire system without any restriction (50000 steps).

Then, each system was gradually heated from 50 to 300 K using a stepwise approach in which the molecules were first simulated for 250 ps in the NVT ensemble, followed by 250 ps of simulation in the NPT ensemble at 1 atm, before increasing the temperature by 50 K. This cycle was repeated until reaching 300 K and, at each step, the restraints were reduced by 2 Kcal/mol. Afterward, the proteins were allowed to relax without constraints for 5 ns at 300 K in the NPT ensemble before launching the production runs. Finally, a production run of 1 μs was carried out in the NPT ensemble at 1 atm and 300 K. A 2 fs integration time step was employed in each step.

The same MDs protocol has been applied to simulate the apo-form of the RORγ receptor (PDB ID 3l0j)[1].

GPBAR1. Each receptor-ligand complex has been embedded in a 94 Å × 94 Å × 94 Å (in '*x*', '*y*' and '*z*' axes) lipid bilayer composed of 1-Palmitoyl-2-oleoylphosphatidylcholine (POPC) and cholesterol with a ratio POPC:cholesterol equal to 7:3 using the membrane-builder tool of CHARMM-GUI.org.[23,24] Each membrane-receptor complex was solvated using the TIP3P water model[25] and neutralized with the addition of 1 Cl^- ion. The ionic strength was kept at 0.15 M by NaCl. The Amber *ff14SB*, GAFF and *lipid14* Amber force fields[21,22,26] were used to parametrize the protein, the ligand, and the lipids, respectively. All simulations were performed with NAMD2.12 code.[20] The SHAKE algorithm was applied to constrain bonds involving hydrogen atoms, and thus integration of 1 fs time step interval until the thermalization at 200 K, then increased to 2 fs time step, was used.

System thermalization was carried out using the same protocol designed for RORγ. Finally, a production run of 1 μs was carried out in the NPT ensemble at 1 atm and 300 K.

***In vivo* assays**

Mouse models of colitis. C57BL6 mice were purchased from Charles River. In the animal facility of the University of Perugia, mice were housed under controlled temperatures (22 °C) and photoperiods (12:12-h light/dark cycle), allowed unrestricted access to standard mouse chow and tap water and allowed to acclimate to these conditions for at least 5 days before inclusion in an experiment. The study was conducted in compliance with Italian law and the protocol was approved by an ethical

committee of the University of Perugia and by a national committee of the Ministry of Health (permission n. 1126/2016-PR and n. 583/2017-PR). The health and body conditions of the animals were monitored daily by the Veterinarian in the animal facility. The study protocol caused minor suffering, however, animals that lost more than 25% of the initial body weight were euthanized. In brief, for induction of colitis mice were fasted for 1 day (day called −1). The day after (day 0) mice were anesthetized, and a 3.5 F catheter inserted into the colon such that the tip was 4 cm proximal to the anus. To induce colitis, 1 mg of TNBS (Sigma Chemical Co., St Louis, MO, USA) in 50% ethanol was administered via catheter into the lumen using a 1 mL syringe (injection volume of 100 μL); control mice received 50% ethanol alone. When prompted by the experimental design the compound **7** was administered by gavage (o.s.) at the dose of 10, 20 or 30 mg/kg daily starting from day 0. In another experimental set mice were administered daily by gavage (o.s.) with BAR501 30 mg/kg, a selective GPBAR1 agonist, or ML209 20 mg/kg, a selective RORγt inverse agonist. Animals were monitored daily for appearance of diarrhea, loss of body weight, presence of blood in the stool and survival. At the end of the experiment, 4 days after the administration of TNBS, surviving mice were sacrificed and the colon were excised.

The severity of colitis was measured each day for each mouse by analyzing the body weight lost, the occult blood and stool consistency. Each parameter was scored from 0 to 4 and the sum represents the Colitis Disease Activity Index (CDAI). The scoring system was as following: percent of body weight loss: none = 0; 1–5% = 1; 5–10% = 2; 10–20% = 3; >20% = 4. Stool consistency: normal = 0; soft but still formed = 1; very soft = 2; diarrhea = 3; liquid stools that stick to the anus or anal occlusion = 4. Fe-cal blood: none = 0; visible in the stool = 2; severe bleeding with fresh blood around the anus and very present in the stool = 4.

Histopathology. Colon samples (2–3 cm up the anus) were first fixed in 10% Formalin (Bio-Optica Milano S.p.A. Milan, IT), embedded in Paraffin (Bio-Optica Milano S.p.A. Milan, IT), cut into 5-μm-thick sections and then stained with Hematoxylin/Eosin (H&E) (Bio-Optica Milano S.p.A. Milan, IT) for histopathological analysis.

Reverse Transcription of mRNA and Real-Time PCR. RNA was extracted from mouse colon using TRIzol reagent (Invitrogen). After purification from genomic DNA using DNase I (Thermo Fisher Scientific, Waltham, MA, USA), 1 μg of RNA from each sample was reverse transcribed using a FastGene Scriptase Basic Kit (Nippon Genetics Europe) in a 20 μL reaction volume; 50 ng of cDNA was amplified in a 20 μL solution containing 200 nM of each primer and 10 μL of SYBR Select Master Mix (Thermo Fisher Scientific, Waltham, MA, USA). All reactions were performed in triplicate using the following thermal cycling conditions: 3 min at 95 °C, followed by 40 cycles of 95 °C for 15 s, 56 °C for 20 s and 72 °C for 30 s, using a StepOnePlus system (Applied Biosystems, Foster City, CA, USA). The relative mRNA expression was calculated according to the ΔCt method. Primers were designed using the software PRIMER3 (http://frodo.wi.mit.edu/primer3/, accessed on 1 January 2021), using data published in the NCBI database. The primer used for human genes were as following (forward and reverse):

IL-1β for: GTGGCAATGAGGATGACTTG, rev: GGAGATTCGTAGCTGGATGC; IL-6 for: AGTGAGGAACAAGCCAGAGC, rev: CAGGGGTGGTTATTGCATCT; TNF-α for: AGCCCATGTTGTAGCAAACC, rev: TGAGGTACAGGCCCTCTGAT; CD11c for: ACCTCACCGGACTCTGCTT, rev: ATGTCCTGCTCCTGTCTTGG.

The primer used for mouse genes were as following (forward and reverse):

Il-1β for: TGTGAAATGCCACCTTTTGA, rev: GGTCAAAGGTTTGGAAGCAG; Il-6 for: CTTCACAAGTCGGAGGCTTA, rev: TTCTGCAAGTGCATCATCGT; Tnf-α for: GCCTCTTCTCATTCCTGCTT, rev: GAGGCCATTTGGGAACTTCT; Il-10 for: CAGCCGGGAAGACAATAACT, rev: TTGTCCAGCTGGTCCTTTGT; Tgf-β for: TAATGGTGGACCGCAACAAC, rev: ACTGCTTCCCGAATGTCTGA; Cd11b for: GTCAGAGTCTGCCTCCGTGT, rev: CAGGGTCTAAAGCCAGGTCA; Cd38 for: CTGGGCTACATTGCTGATGA, rev: GGGTTGTTGGGACAGTTTTC; Rorc for: CAGCCAGCAGTGTAATGTGG, rev: AACTTGACAGCATCTCGGGA; Il-17A for:

TCCAGAAGGCCCTCAGACTA, rev: TGAGCTTCCCAGATCACAGA; Il-17F for: ATGAAGTGCACCCGTGAAAC, rev: GGTTCTTCCGAGCTGCTACC.

Figure S6. ^{1}H NMR (400 MHz, $CDCl_3$) of compound **1**

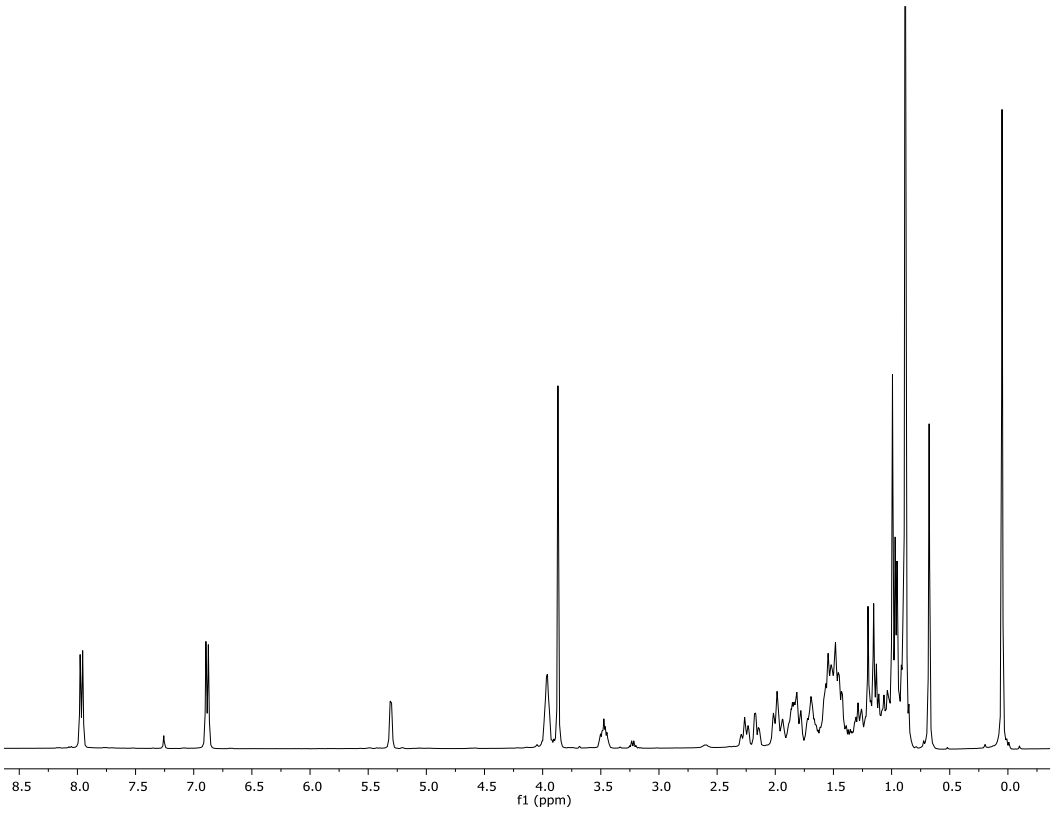

Figure S7. ^{1}H NMR (400 MHz, $CDCl_3$) of compound **2**

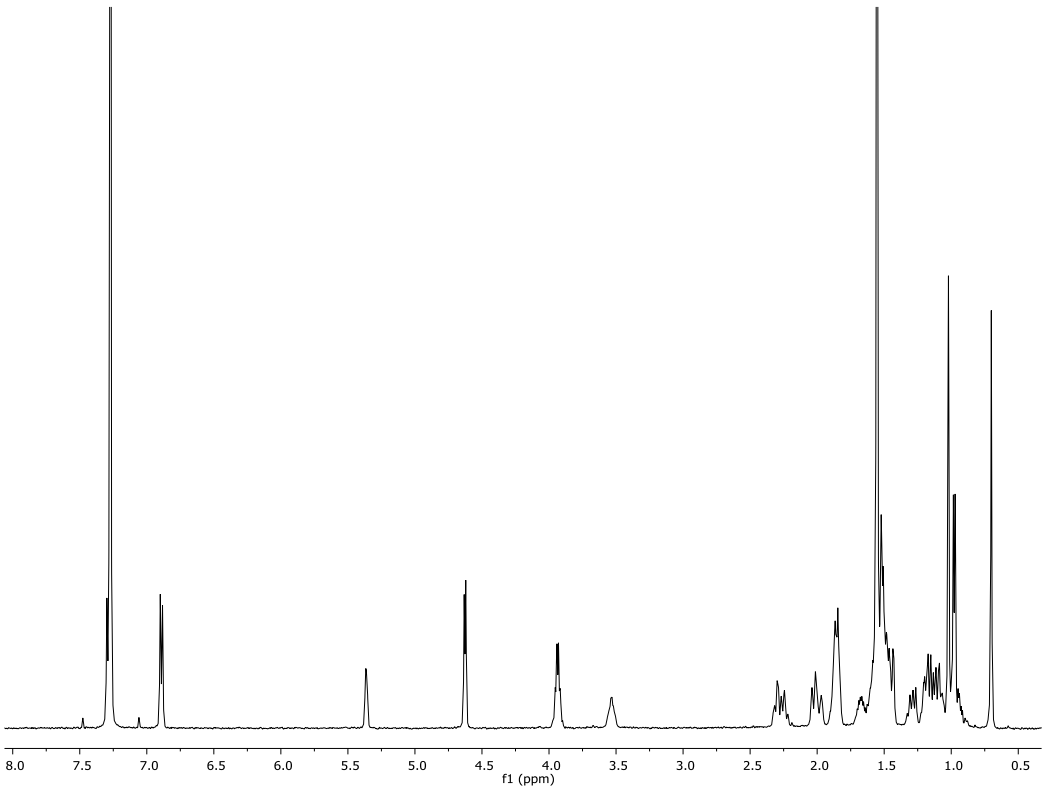

Figure S8. ^{1}H NMR (400 MHz, $CDCl_3$) of compound **3**

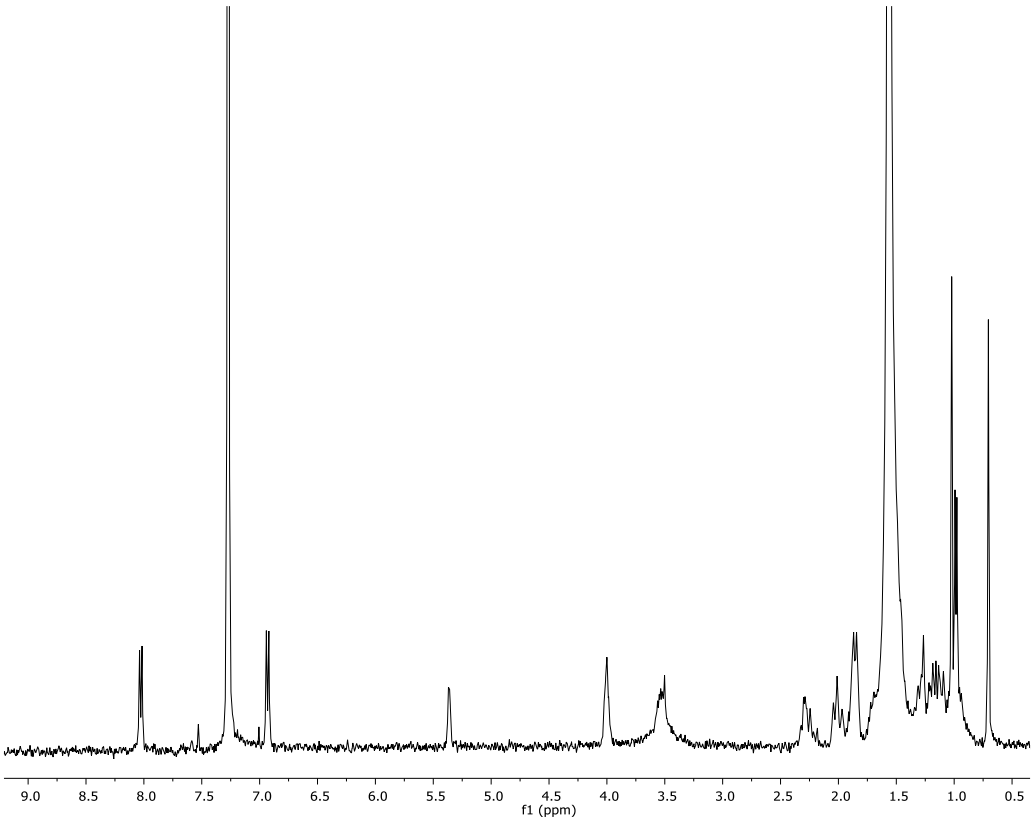

Figure S9. ^{1}H NMR (400 MHz, $CDCl_3$) of compound **4**

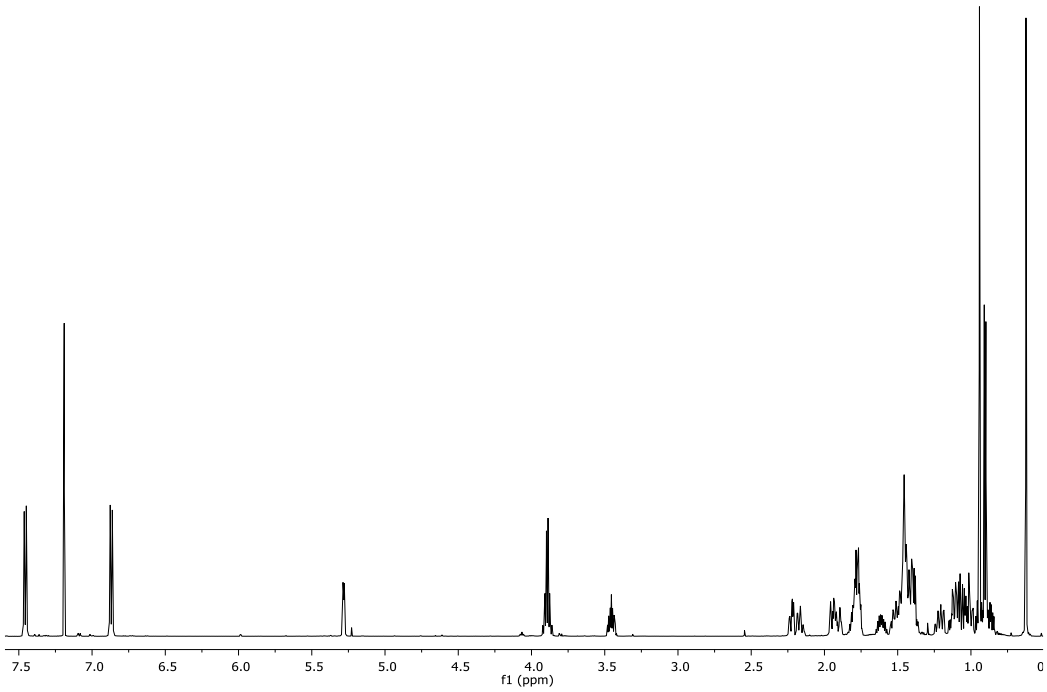

Figure S10. ^{1}H NMR (400 MHz, $CDCl_3$) of compound **5**

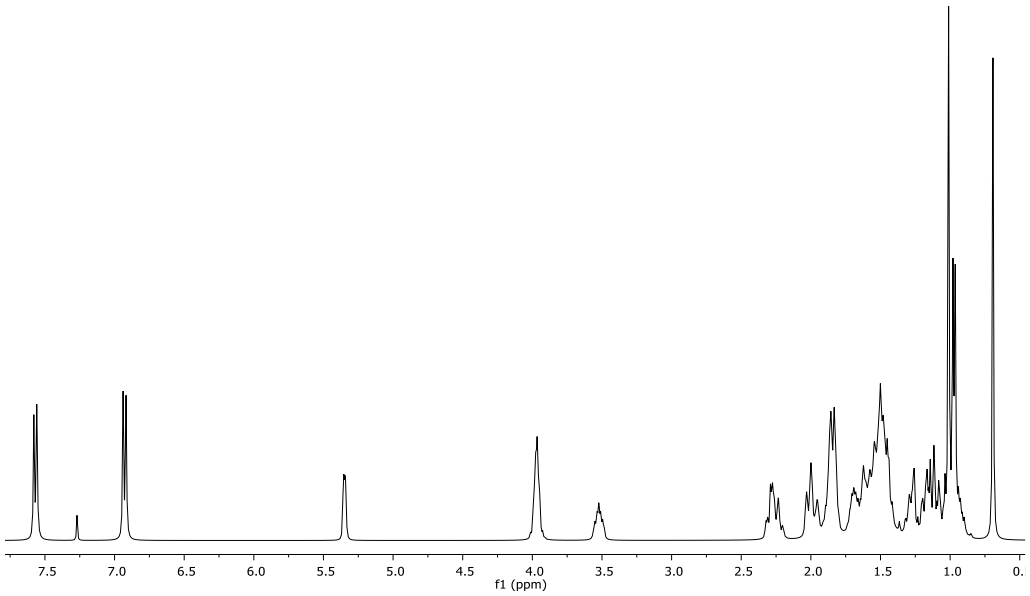

Figure S11. ^{1}H NMR (400 MHz, CD_3OD) of compound **6**

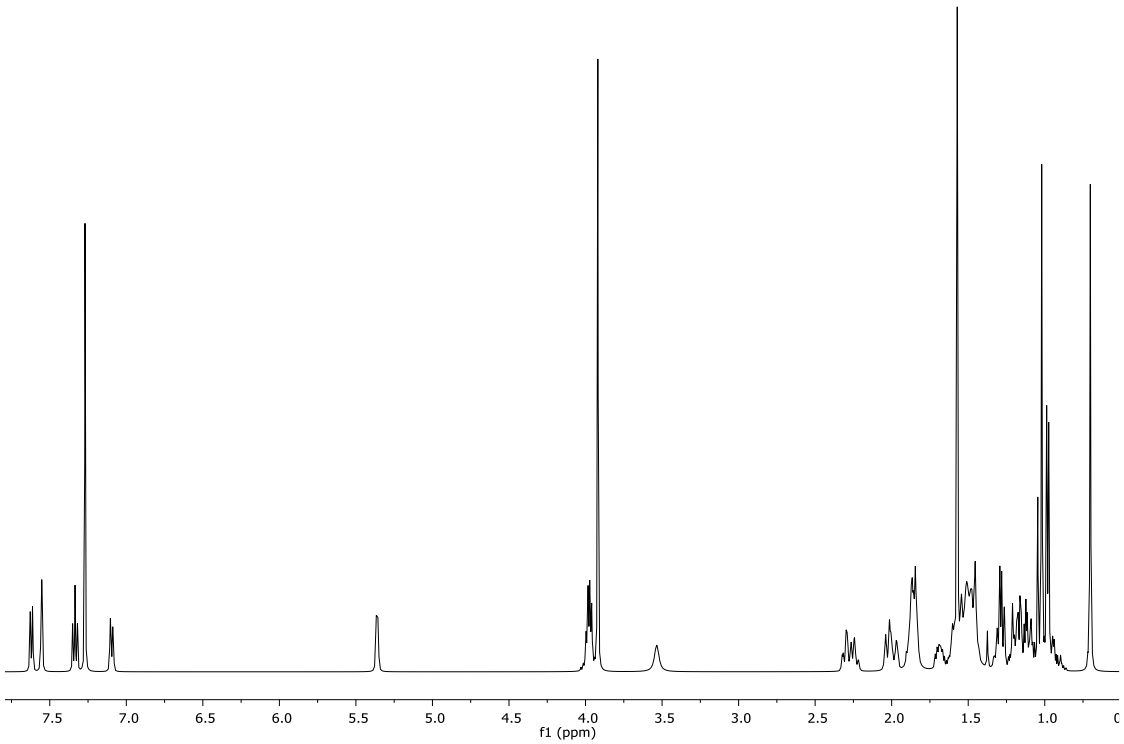

Figure S12. ^{1}H NMR (400 MHz, $CDCl_3$) of compound **7**

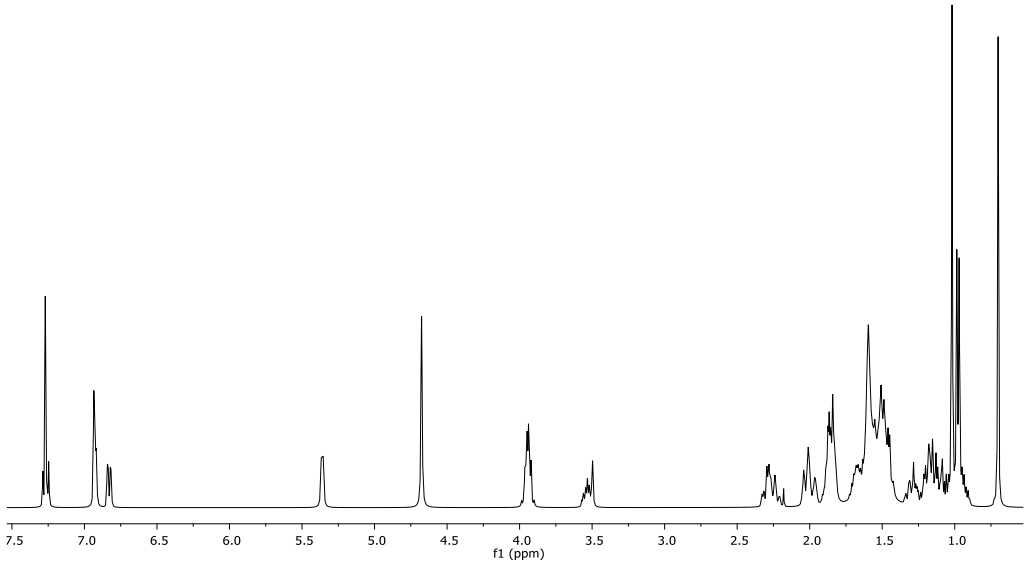

Figure S13. ^{1}H NMR (400 MHz, $CDCl_3$) of compound **8**

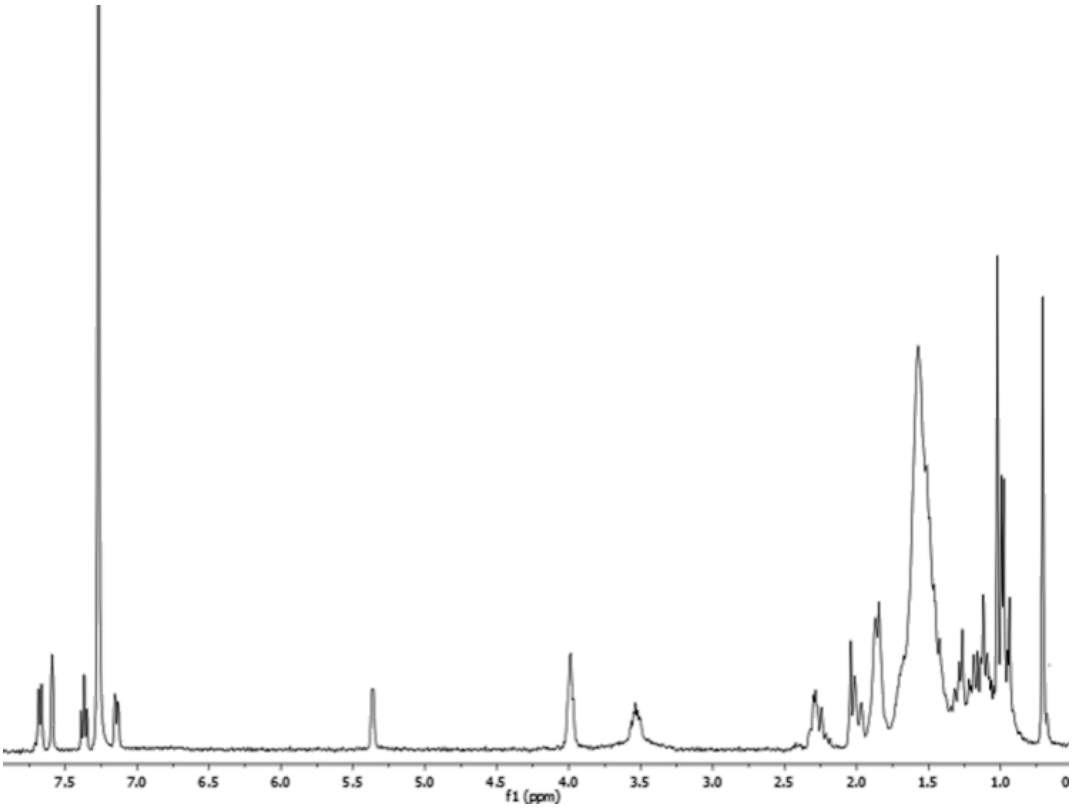

Figure S14. ^{1}H NMR (400 MHz, $CDCl_3$) of compound **9**

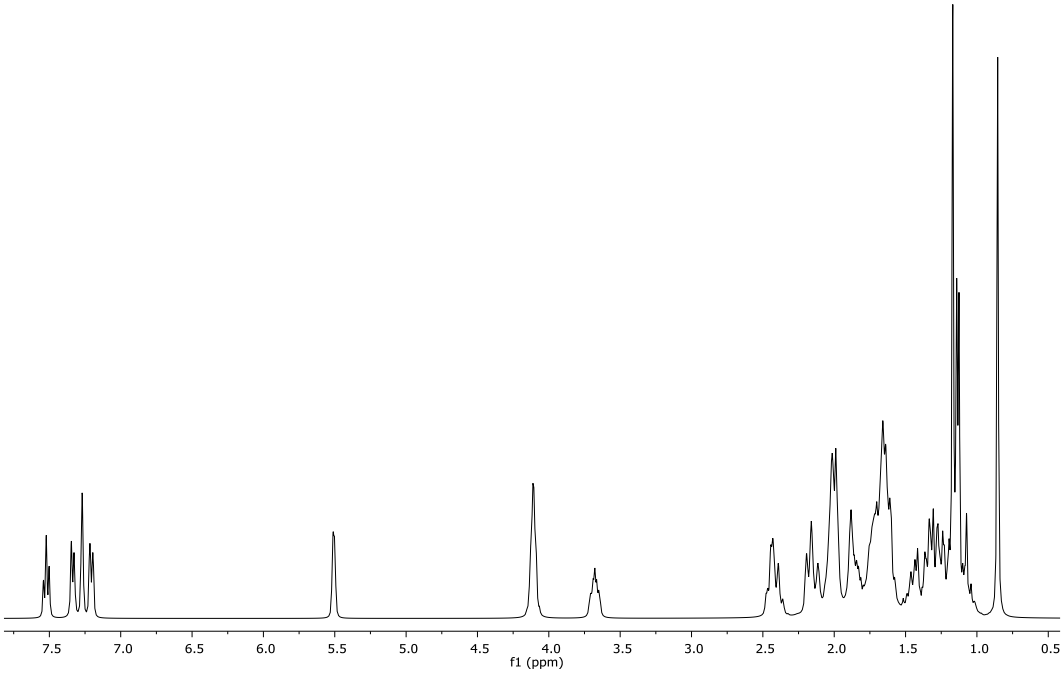

Figure S15. ^{1}H NMR (400 MHz, $CDCl_3$) of compound **10**

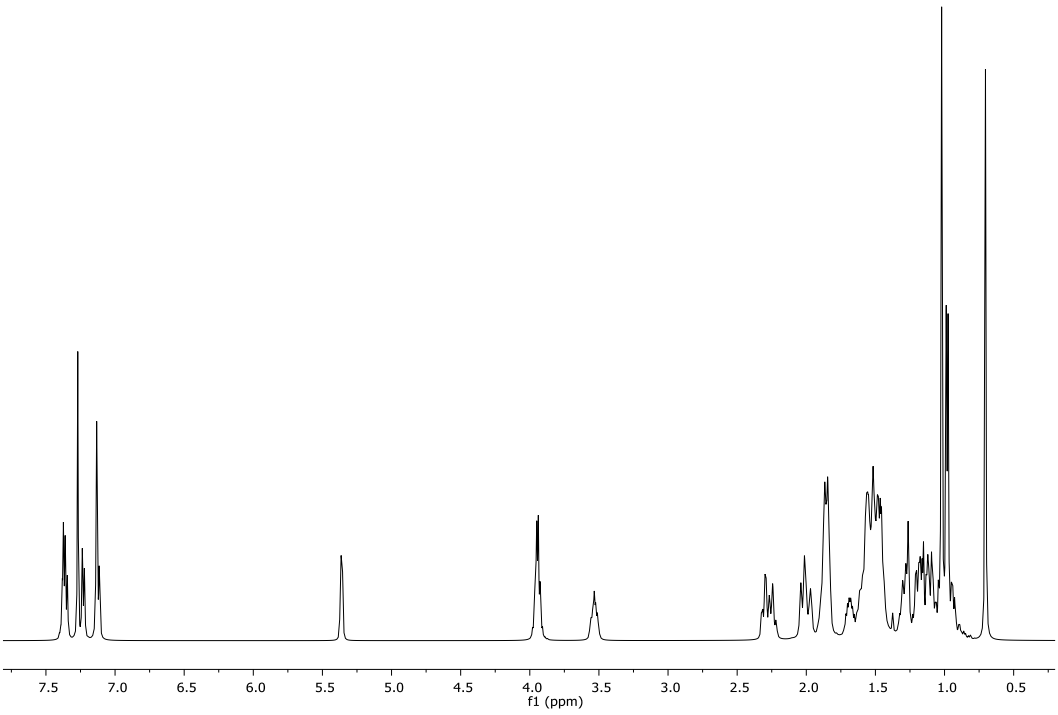

Figure S16. ^{1}H NMR (400 MHz, $CDCl_3$) of compound **11**

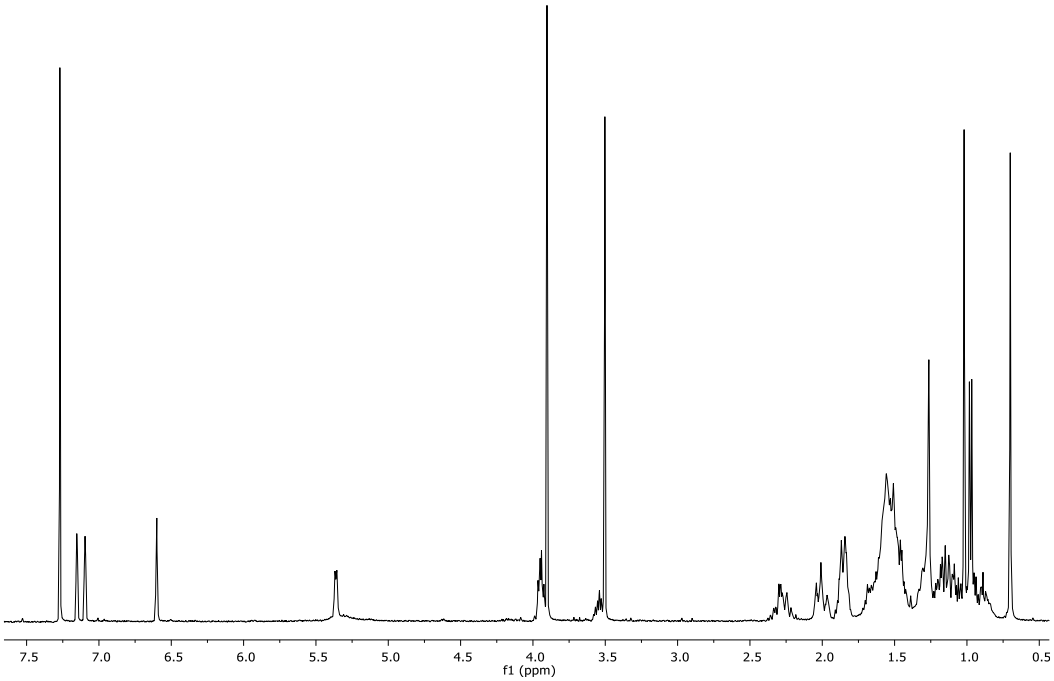

Figure S17. ^{1}H NMR (400 MHz, $CDCl_3$) of compound **12**

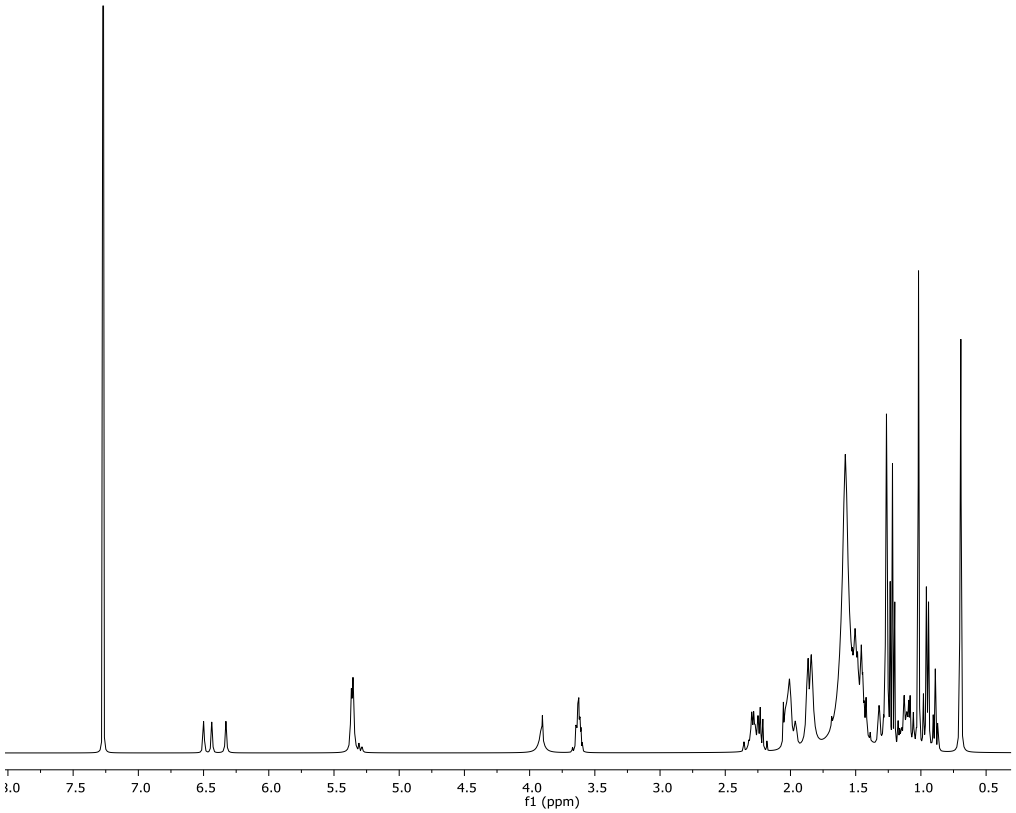

Figure S18. ^{1}H NMR (400 MHz, CD_3OD) of compound **13**

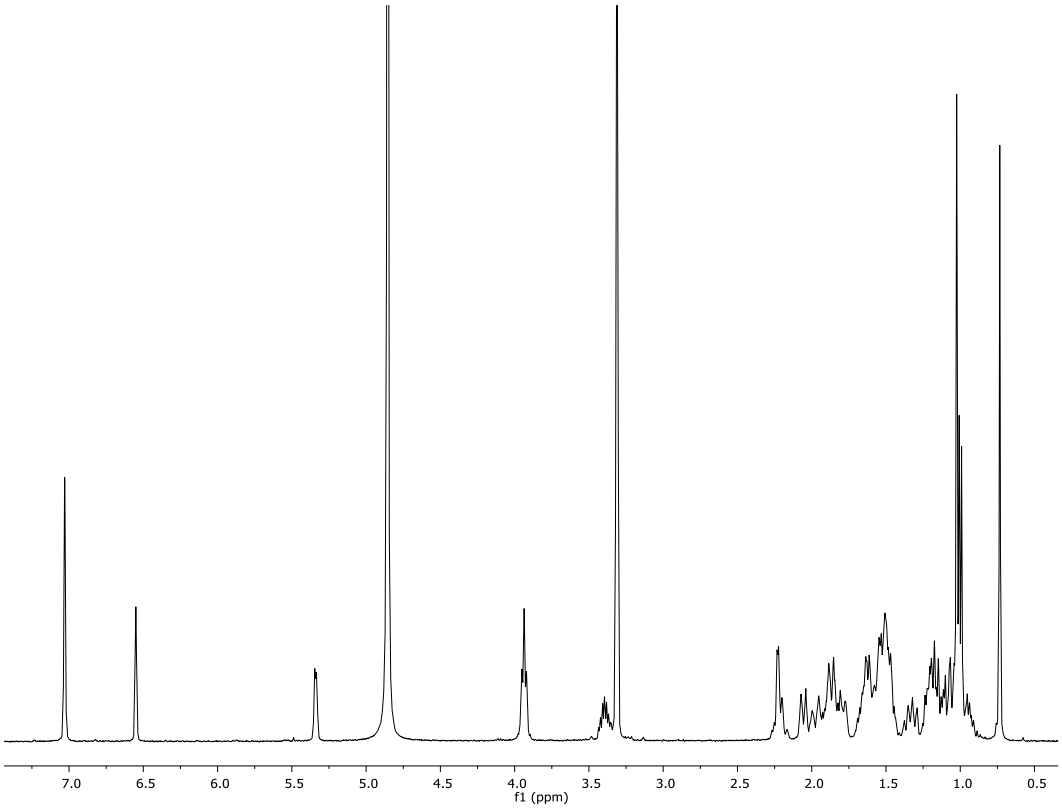

Figure S19. ^{1}H NMR (400 MHz, $CDCl_3$) of compound **14**

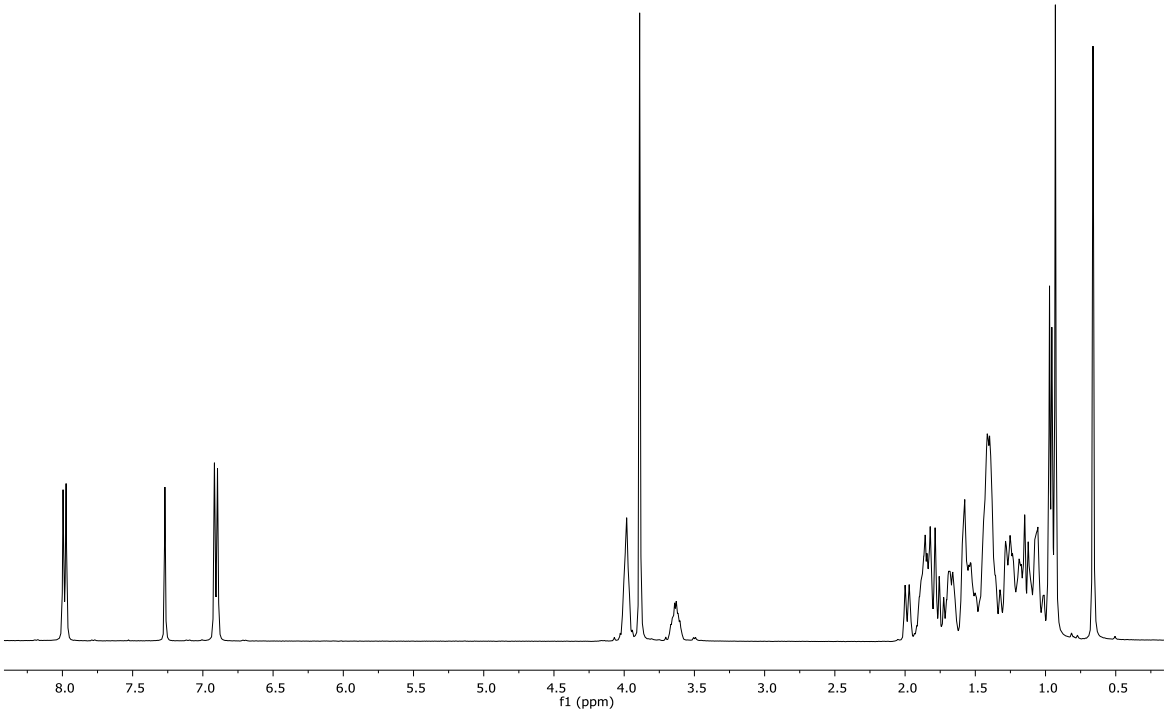

Figure S20. ^{1}H NMR (400 MHz, $CDCl_3$) of compound **15**

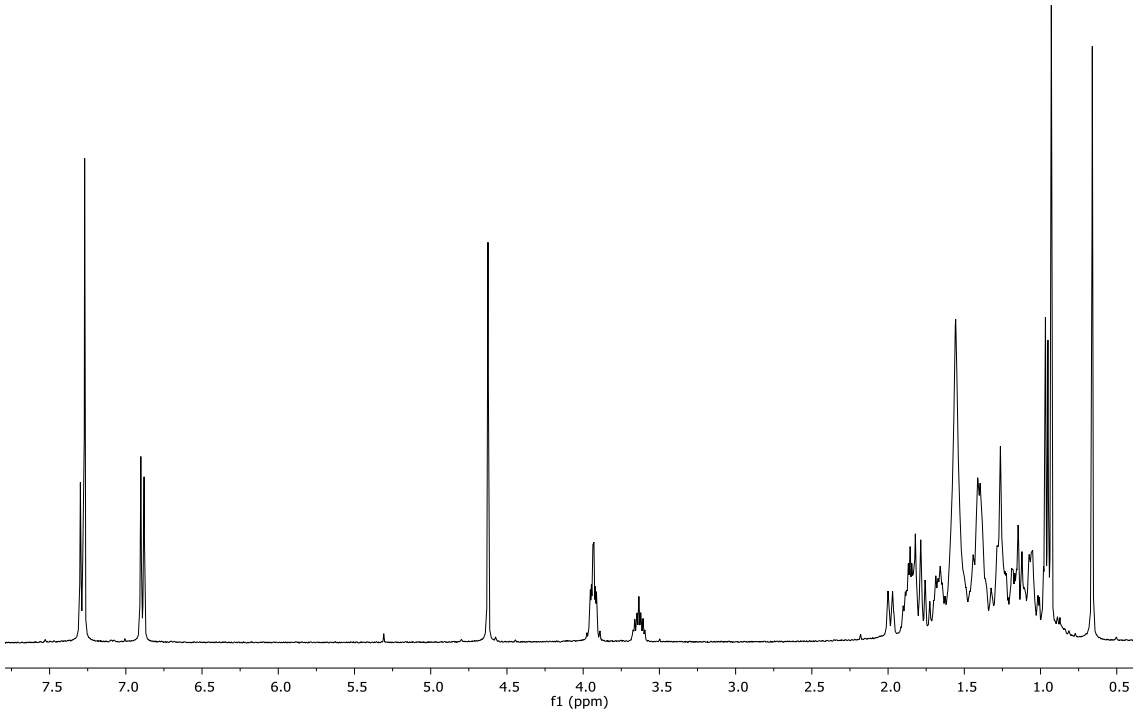

Figure S21. ^{1}H NMR (400 MHz, $CDCl_3$) of compound **16**

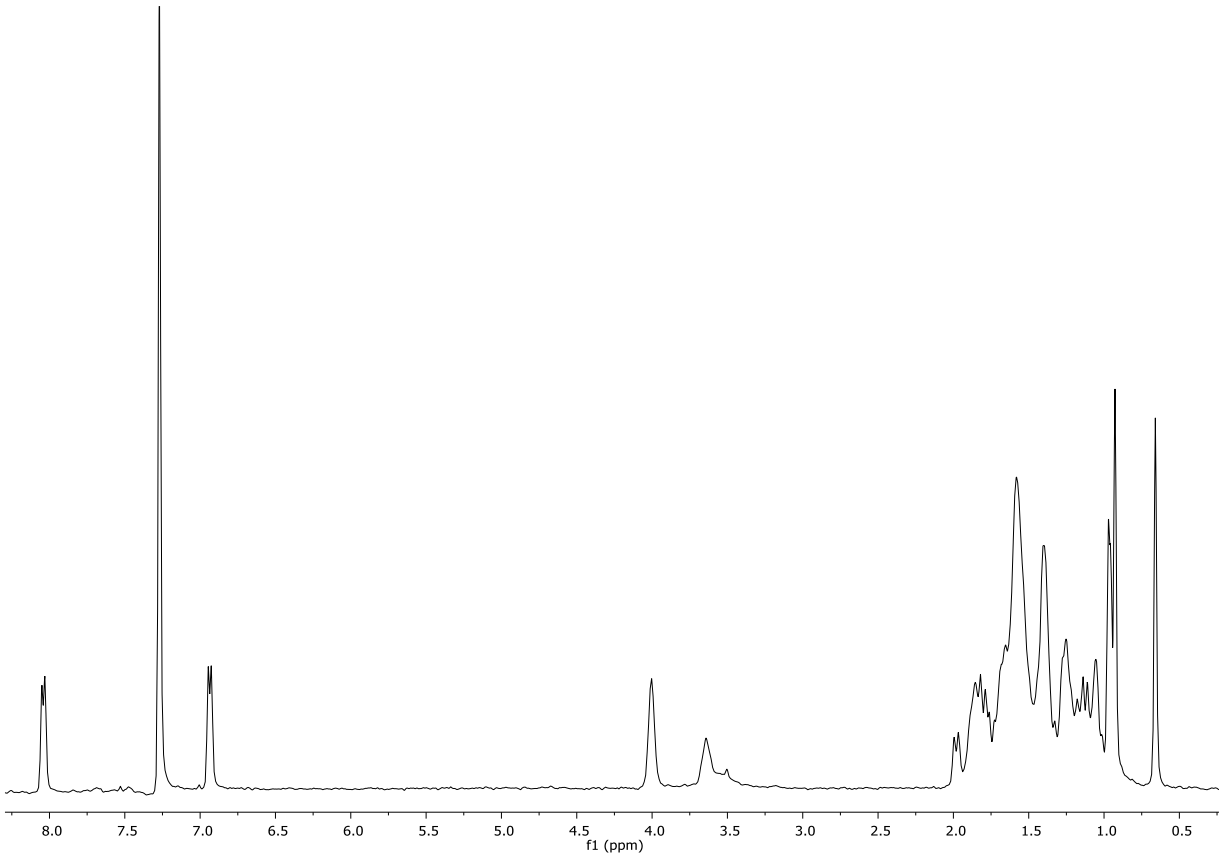

Figure S22. ^{1}H NMR (400 MHz, $CDCl_3$) of compound **17**

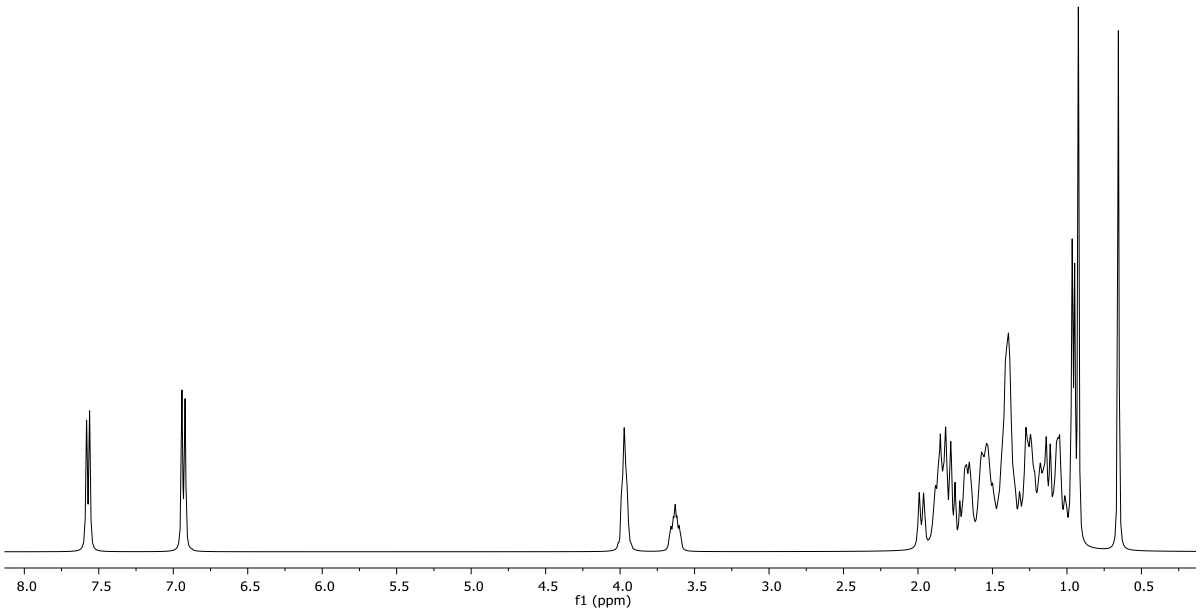

Figure S23. ^{1}H NMR (400 MHz, $CDCl_3$) of compound **18**

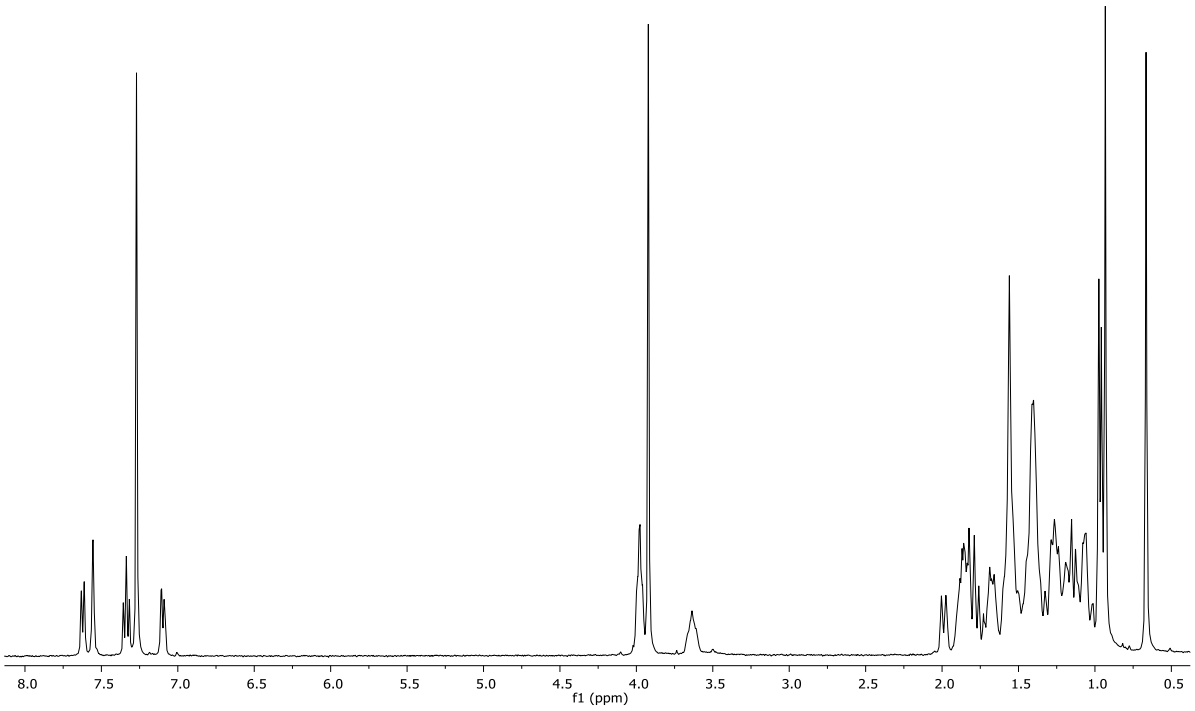

Figure S24. ^{1}H NMR (400 MHz, $CDCl_3$) of compound **19**

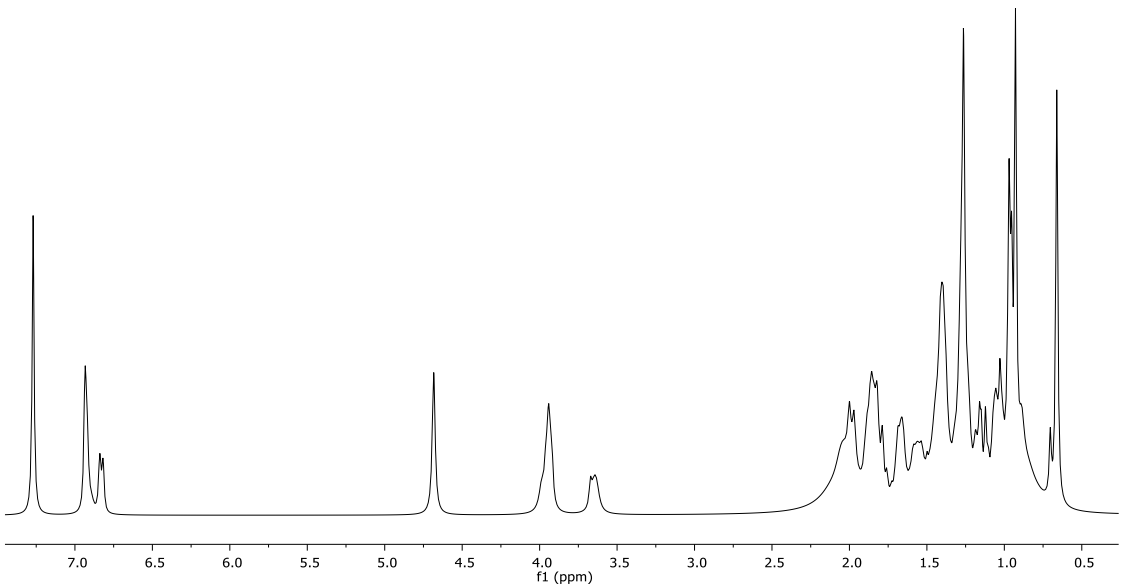

Figure S25. ^{1}H NMR (400 MHz, $CDCl_3$) of compound **20**

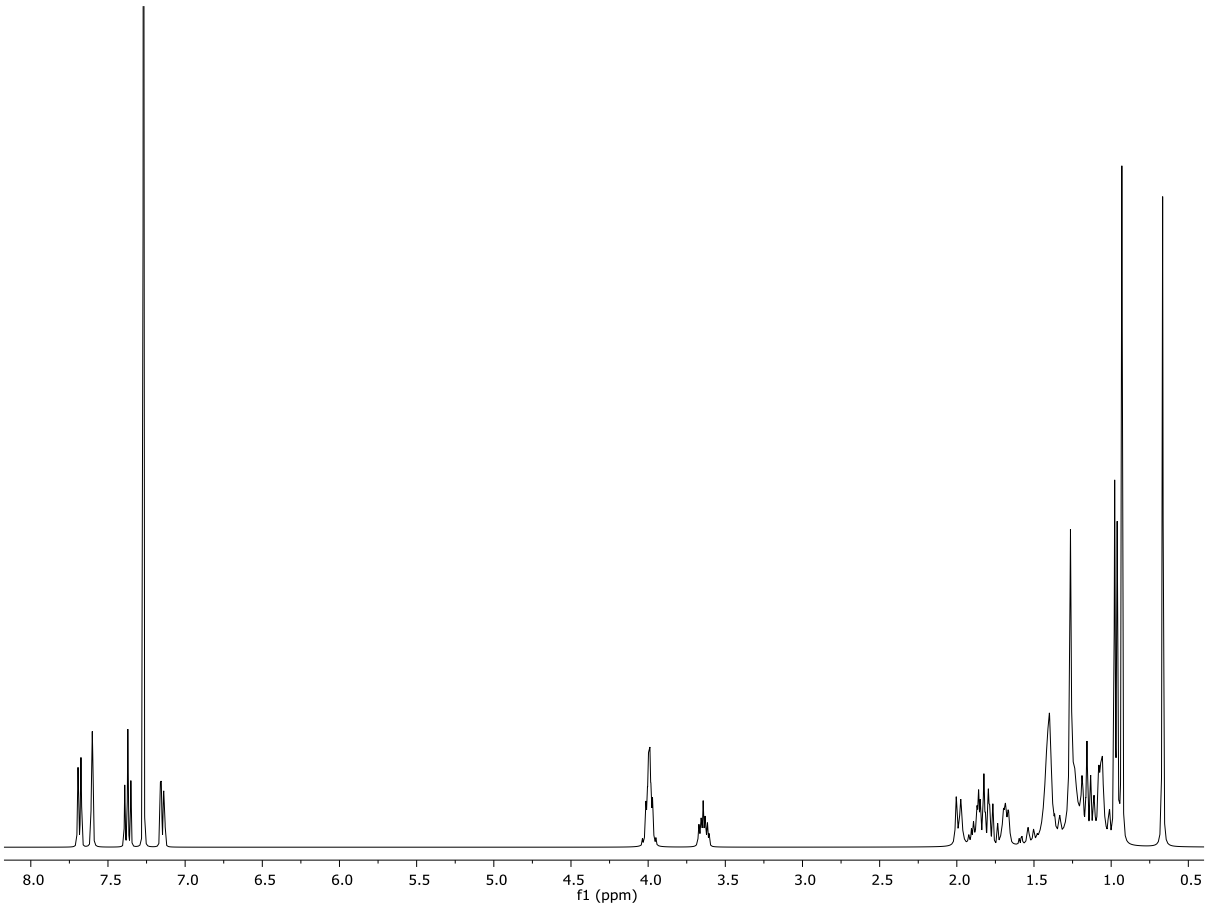

Figure S26. ^{1}H NMR (400 MHz, $CDCl_3$) of compound **21**

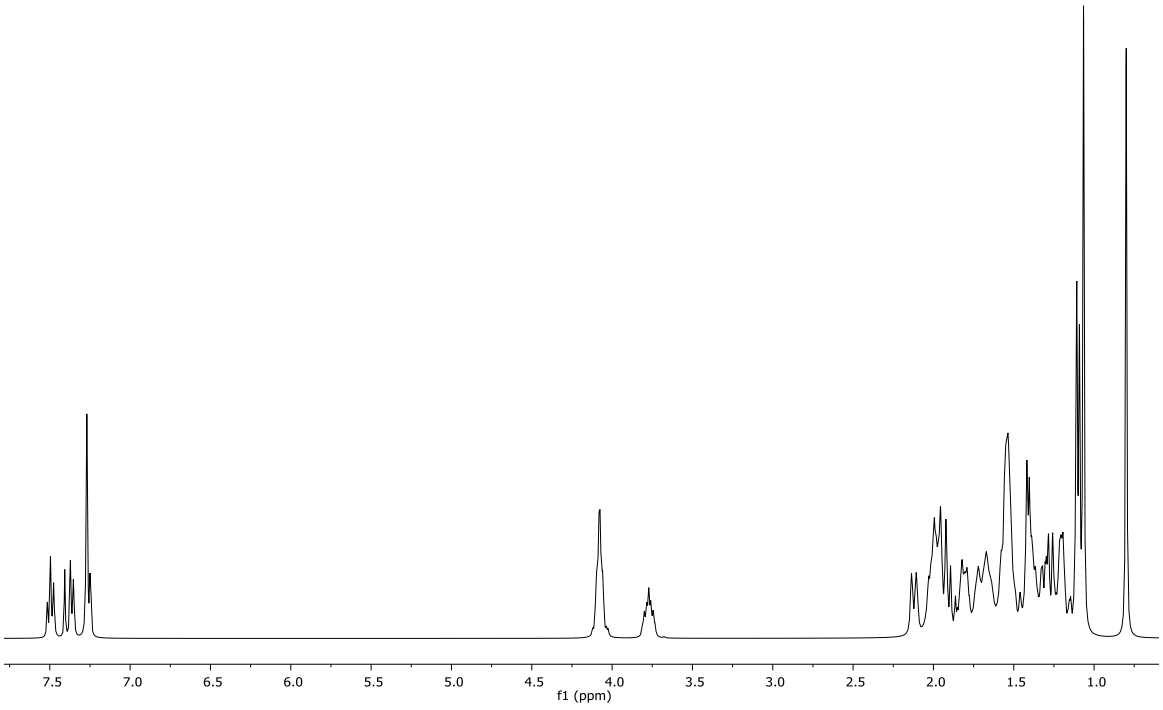

Figure S27. HPLC trace of compound **3**

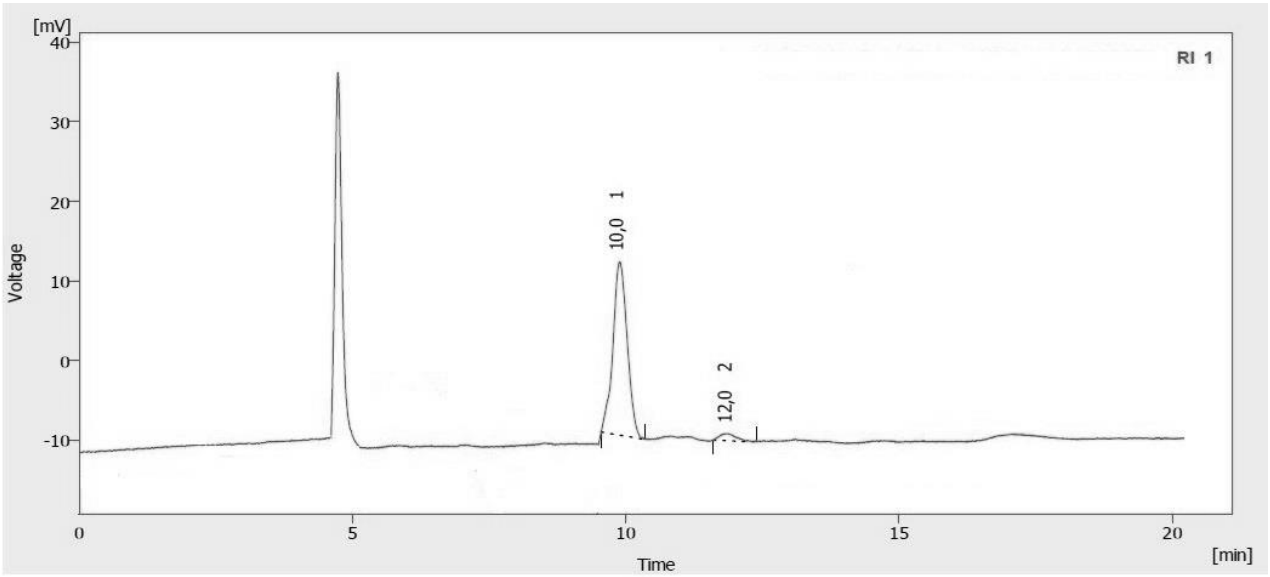

	Reten. Time [min]	Area [mV.s]	Height [mV]	Area [%]	Height [%]	W05 [min]	Compound Name
1	10,039	395,897	21,801	95,3	95,8	0,28	
2	12,025	19,432	0,947	4,7	4,2	0,29	
	Total	415,329	22,748	100,0	100,0		

Figure S28. HPLC trace of compound **7**

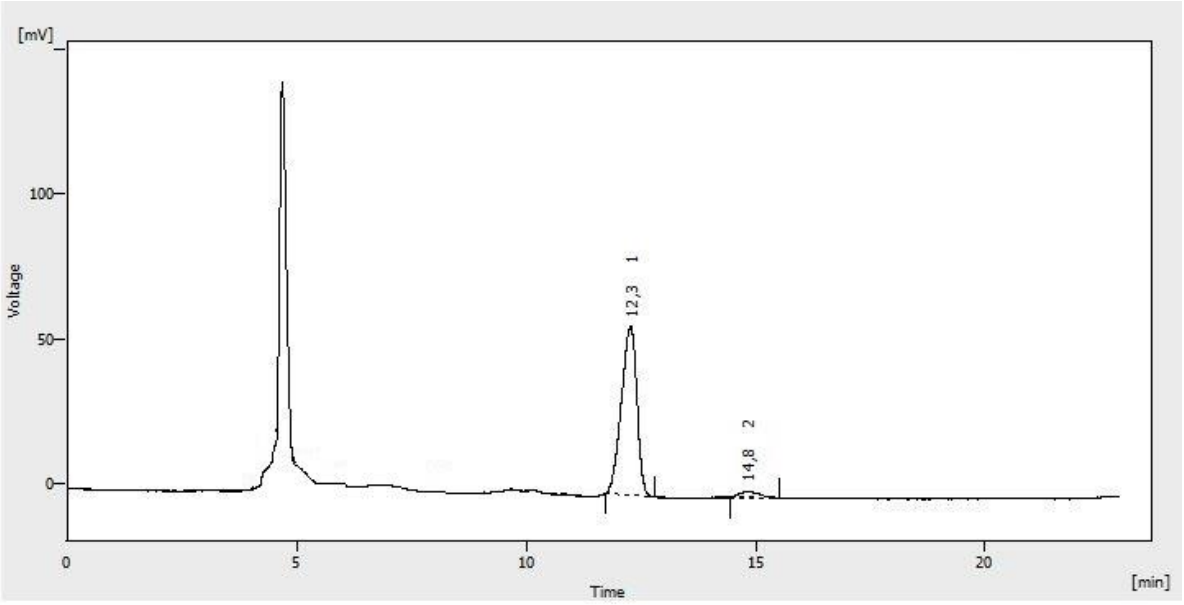

	Reten. Time [min]	Area [mV.s]	Height [mV]	Area [%]	Height [%]	W05 [min]	Compound Name
1	12,276	1370,204	58,182	95,6	96,5	0,37	
2	14,809	63,400	2,136	4,4	3,5	0,46	
	Total	1433,604	60,317	100,0	100,0		

References

(1) Jin, L.; Martynowski, D.; Zheng, S.; Wada, T.; Xie, W.; Li, Y. Structural Basis for Hydroxycholesterols as Natural Ligands of Orphan Nuclear Receptor RORγ. *Mol Endocrinol* **2010**, *24* (5), 923–929. https://doi.org/10.1210/me.2009-0507.

(2) Kallen, J.; Izaac, A.; Be, C.; Arista, L.; Orain, D.; Kaupmann, K.; Guntermann, C.; Hoegenauer, K.; Hintermann, S. Structural States of RORγt: X-Ray Elucidation of Molecular Mechanisms and Binding Interactions for Natural and Synthetic Compounds. *ChemMedChem* **2017**, *12* (13), 1014–1021. https://doi.org/10.1002/cmdc.201700278.

(3) di Leva, F. S.; Festa, C.; Renga, B.; Sepe, V.; Novellino, E.; Fiorucci, S.; Zampella, A.; Limongelli, V. Structure-Based Drug Design Targeting the Cell Membrane Receptor GPBAR1: Exploiting the Bile Acid Scaffold towards Selective Agonism. *Sci Rep* **2015**, *5* (1), 16605. https://doi.org/10.1038/srep16605.

(4) D'Amore, C.; di Leva, F. S.; Sepe, V.; Renga, B.; del Gaudio, C.; D'Auria, M. V.; Zampella, A.; Fiorucci, S.; Limongelli, V. Design, Synthesis, and Biological Evaluation of Potent Dual Agonists of Nuclear and Membrane Bile Acid Receptors. *J Med Chem* **2014**, *57* (3), 937–954. https://doi.org/10.1021/jm401873d.

(5) Sepe, V.; Renga, B.; Festa, C.; D'Amore, C.; Masullo, D.; Cipriani, S.; di Leva, F. S.; Monti, M. C.; Novellino, E.; Limongelli, V.; Zampella, A.; Fiorucci, S. Modification on Ursodeoxycholic Acid (UDCA) Scaffold. Discovery of Bile Acid Derivatives As Selective Agonists of Cell-Surface G-Protein Coupled Bile Acid Receptor 1 (GP-BAR1). *J Med Chem* **2014**, *57* (18), 7687–7701. https://doi.org/10.1021/jm500889f.

(6) Gertzen, C. G. W.; Spomer, L.; Smits, S. H. J.; Häussinger, D.; Keitel, V.; Gohlke, H. Mutational Mapping of the Transmembrane Binding Site of the G-Protein Coupled Receptor TGR5 and Binding Mode Prediction of TGR5 Agonists. *Eur J Med Chem* **2015**, *104*, 57–72. https://doi.org/10.1016/j.ejmech.2015.09.024.

(7) Sepe, V.; Ummarino, R.; D'Auria, M. V.; Mencarelli, A.; D'Amore, C.; Renga, B.; Zampella, A.; Fiorucci, S. Total Synthesis and Pharmacological Characterization of Solomonsterol A, a Potent Marine Pregnane-X-Receptor Agonist Endowed with Anti-Inflammatory Activity. *J Med Chem* **2011**, *54* (13), 4590–4599. https://doi.org/10.1021/jm200241s.

(8) Anzini, M.; Braile, C.; Valenti, S.; Cappelli, A.; Vomero, S.; Marinelli, L.; Limongelli, V.; Novellino, E.; Betti, L.; Giannaccini, G.; Lucacchini, A.; Ghelardini, C.; Norcini, M.; Makovec, F.; Giorgi, G.; Ian Fryer, R. Ethyl 8-Fluoro-6-(3-Nitrophenyl)-4 *H* -Imidazo[1,5- *a*][1,4]Benzodiazepine-3-Carboxylate as Novel, Highly Potent, and Safe Antianxiety Agent. *J Med Chem* **2008**, *51* (15), 4730–4743. https://doi.org/10.1021/jm8002944.

(9) Anzini, M.; Valenti, S.; Braile, C.; Cappelli, A.; Vomero, S.; Alcaro, S.; Ortuso, F.; Marinelli, L.; Limongelli, V.; Novellino, E.; Betti, L.; Giannaccini, G.; Lucacchini, A.; Daniele, S.; Martini, C.; Ghelardini, C.; di Cesare Mannelli, L.; Giorgi, G.; Mascia, M. P.; Biggio, G. New Insight into the Central Benzodiazepine Receptor–Ligand Interactions: Design, Synthesis, Biological Evaluation, and Molecular Modeling of 3-Substituted 6-Phenyl-4 *H* -Imidazo[1,5- *a*][1,4]Benzodiazepines and Related Compounds. *J Med Chem* **2011**, *54* (16), 5694–5711. https://doi.org/10.1021/jm2001597.

(10) Nuti, E.; Casalini, F.; Avramova, S. I.; Santamaria, S.; Fabbi, M.; Ferrini, S.; Marinelli, L.; la Pietra, V.; Limongelli, V.; Novellino, E.; Cercignani, G.; Orlandini, E.; Nencetti, S.; Rossello, A. Potent Arylsulfonamide Inhibitors of Tumor Necrosis Factor-α Converting Enzyme Able to Reduce Activated Leukocyte Cell Adhesion Molecule Shedding in Cancer Cell Models. *J Med Chem* **2010**, *53* (6), 2622–2635. https://doi.org/10.1021/jm901868z.

(11) Deplano, A.; Morgillo, C. M.; Demurtas, M.; Björklund, E.; Cipriano, M.; Svensson, M.; Hashemian, S.; Smaldone, G.; Pedone, E.; Luque, F. J.; Cabiddu, M. G.; Novellino, E.; Fowler, C. J.; Catalanotti, B.; Onnis, V. Novel Propanamides as Fatty Acid Amide Hydrolase Inhibitors. *Eur J Med Chem* **2017**, *136*, 523–542. https://doi.org/10.1016/j.ejmech.2017.05.033.

(12) Biagioli, M.; Carino, A.; Marchianò, S.; Roselli, R.; di Giorgio, C.; Bordoni, M.; Fiorucci, C.; Sepe, V.; Conflitti, P.; Limongelli, V.; Distrutti, E.; Baldoni, M.; Zampella, A.; Fiorucci, S. Identification of Cysteinyl-Leukotriene-Receptor 1 Antagonists as Ligands for the Bile Acid Receptor GPBAR1. *Biochem Pharmacol* **2020**, *177*, 113987. https://doi.org/10.1016/j.bcp.2020.113987.

(13) Schrödinger Release 2019-1: Maestro, New York, NY: Schrödinger, LLC, 2019.

(14) Shelley, J. C.; Cholleti, A.; Frye, L. L.; Greenwood, J. R.; Timlin, M. R.; Uchimaya, M. Epik: A Software Program for PK a Prediction and Protonation State Generation for Drug-like Molecules. *J Comput Aided Mol Des* **2007**, *21* (12), 681–691. https://doi.org/10.1007/s10822-007-9133-z.
(15) Grippo, L.; Lucidi, S. A Globally Convergent Version of the Polak-Ribière Conjugate Gradient Method. *Math Program* **1997**, *78* (3), 375–391. https://doi.org/10.1007/BF02614362.
(16) Glide, Version 7.1. New York, NY: Schrödinger, LLC, 2019.
(17) Halgren, T. A.; Murphy, R. B.; Friesner, R. A.; Beard, H. S.; Frye, L. L.; Pollard, W. T.; Banks, J. L. Glide: A New Approach for Rapid, Accurate Docking and Scoring. 2. Enrichment Factors in Database Screening. *J Med Chem* **2004**, *47* (7), 1750–1759. https://doi.org/10.1021/jm030644s.
(18) Friesner, R. A.; Banks, J. L.; Murphy, R. B.; Halgren, T. A.; Klicic, J. J.; Mainz, D. T.; Repasky, M. P.; Knoll, E. H.; Shelley, M.; Perry, J. K.; Shaw, D. E.; Francis, P.; Shenkin, P. S. Glide: A New Approach for Rapid, Accurate Docking and Scoring. 1. Method and Assessment of Docking Accuracy. *J Med Chem* **2004**, *47* (7), 1739–1749. https://doi.org/10.1021/jm0306430.
(19) Banks, J. L.; Beard, H. S.; Cao, Y.; Cho, A. E.; Damm, W.; Farid, R.; Felts, A. K.; Halgren, T. A.; Mainz, D. T.; Maple, J. R.; Murphy, R.; Philipp, D. M.; Repasky, M. P.; Zhang, L. Y.; Berne, B. J.; Friesner, R. A.; Gallicchio, E.; Levy, R. M. Integrated Modeling Program, Applied Chemical Theory (IMPACT). *J Comput Chem* **2005**, *26* (16), 1752–1780. https://doi.org/10.1002/jcc.20292.
(20) Phillips, J. C.; Braun, R.; Wang, W.; Gumbart, J.; Tajkhorshid, E.; Villa, E.; Chipot, C.; Skeel, R. D.; Kalé, L.; Schulten, K. Scalable Molecular Dynamics with NAMD. *J Comput Chem* **2005**, *26* (16), 1781–1802. https://doi.org/10.1002/jcc.20289.
(21) Maier, J. A.; Martinez, C.; Kasavajhala, K.; Wickstrom, L.; Hauser, K. E.; Simmerling, C. Ff14SB: Improving the Accuracy of Protein Side Chain and Backbone Parameters from Ff99SB. *J Chem Theory Comput* **2015**, *11* (8), 3696–3713. https://doi.org/10.1021/acs.jctc.5b00255.
(22) Wang, J.; Wolf, R. M.; Caldwell, J. W.; Kollman, P. A.; Case, D. A. Development and Testing of a General Amber Force Field. *J Comput Chem* **2004**, *25* (9), 1157–1174. https://doi.org/10.1002/jcc.20035.
(23) Jo, S.; Kim, T.; Iyer, V. G.; Im, W. CHARMM-GUI: A Web-Based Graphical User Interface for CHARMM. *J Comput Chem* **2008**, *29* (11), 1859–1865. https://doi.org/10.1002/jcc.20945.
(24) Jo, S.; Lim, J. B.; Klauda, J. B.; Im, W. CHARMM-GUI Membrane Builder for Mixed Bilayers and Its Application to Yeast Membranes. *Biophys J* **2009**, *97* (1), 50–58. https://doi.org/10.1016/j.bpj.2009.04.013.
(25) Jorgensen, W. L.; Chandrasekhar, J.; Madura, J. D.; Impey, R. W.; Klein, M. L. Comparison of Simple Potential Functions for Simulating Liquid Water. *J Chem Phys* **1983**, *79* (2), 926–935. https://doi.org/10.1063/1.445869.
(26) Dickson, C. J.; Madej, B. D.; Skjevik, Å. A.; Betz, R. M.; Teigen, K.; Gould, I. R.; Walker, R. C. Lipid14: The Amber Lipid Force Field. *J Chem Theory Comput* **2014**, *10* (2), 865–879. https://doi.org/10.1021/ct4010307.